JOHN BARNARD
& STEVEN LUND
USPAS JANUARY 2004

AN APPLICATION OF INTENSE BEAMS

EXAMPLE:

1. HEAVY ION FUSION
   - REQUIREMENTS
   - TARGETS FOR ICF
   - ACCELERATOR
   - DRIFT COMPRESSION
   - FINAL FOCUS
     - PREDICTING SPOT SIZE
   - EXPERIMENTS

National® Brand 42-182 100 SHEETS Made in U.S.A.

Inertial Fusion Energy (IFE) power plants of the future will consist of four parts

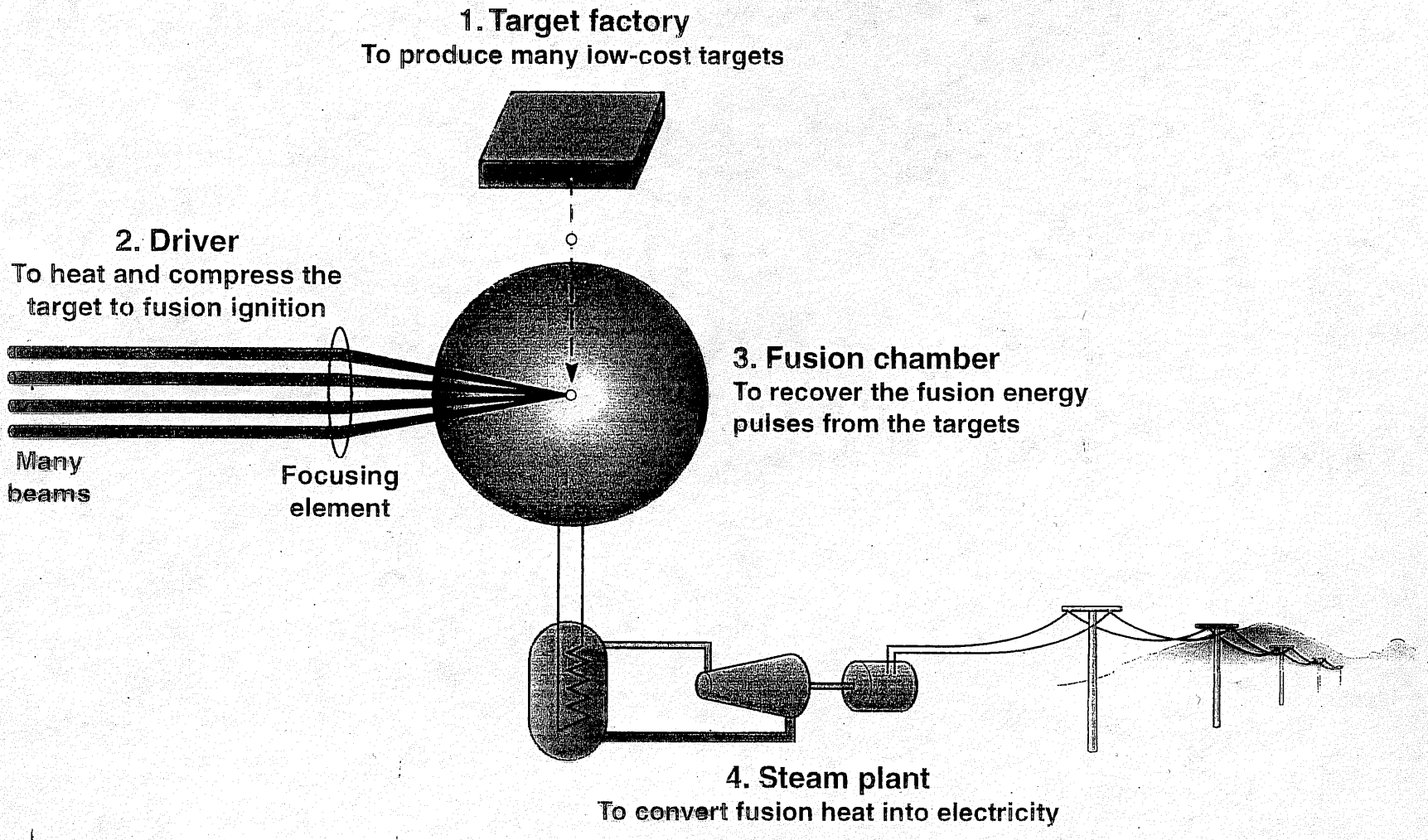

A power-plant driver would fire about five targets per second to produce as much electricity as today's 1000-megawatt power plant

Heavy Ion Fusion provides an attractive approach to long term energy production

Fusion offers an inexaustible, long term solution to the problem of future energy supplies free from long-lived radioactive by-products and greenhouse CO_2.

Inertial Confinement Fusion (ICF) uses laser or particle beams to implode a target, raising the temperature and density of the fuel, creating the conditions necessary for the following reaction:

$$D + T \rightarrow n\ (14.06\ MeV) + He^4\ (3.52\ MeV)\ .$$

Heavy ion accelerators are a strong candidate for inertial fusion *energy production* (IFE) because of:

- High efficiency
- High repetition rate
- Survivability of final lens
- Favorable target illumination geometry

Focusability at the target is key scientific issue

Conditions of beam at target are set by hohlraum and implosion physics

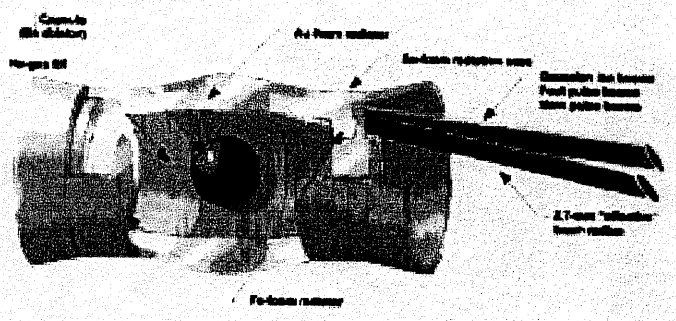

Energy in pulse: ~ 3 to 6 MJ

Duration of main pulse: ~ 8 to 10 ns

Duration of foot pulse: ~ 30 ns

Spot radius: ~ 1.5 to 3 mm

Transverse and longitudinal compression are required to meet target specifications.

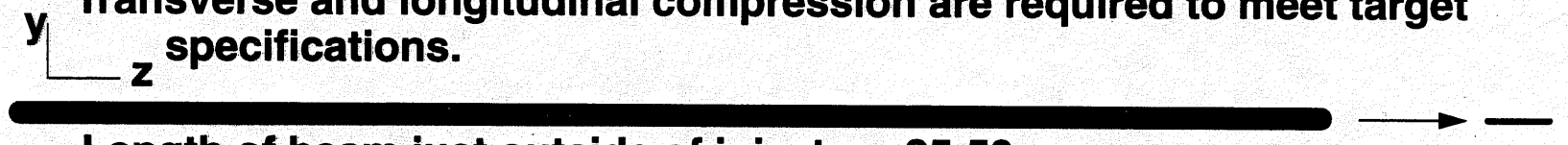

Length of beam just outside of injector ~25-50 m

At target ~ 0.5 - 1 m

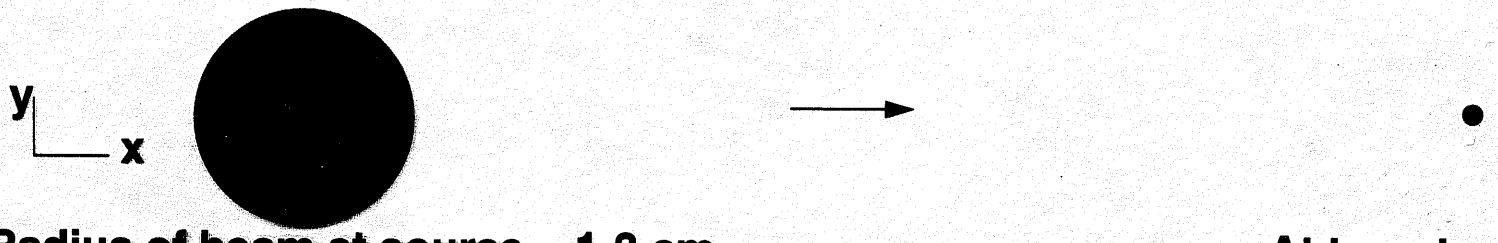

Radius of beam at source ~ 1-3 cm

At target ~ 1.5-3 mm

Compression factors of 10 to 50 in both longitudinal and transverse directions are required.

In the distributed radiator design, low-density foam walls are in approximate pressure balance with a low-Z gas fill

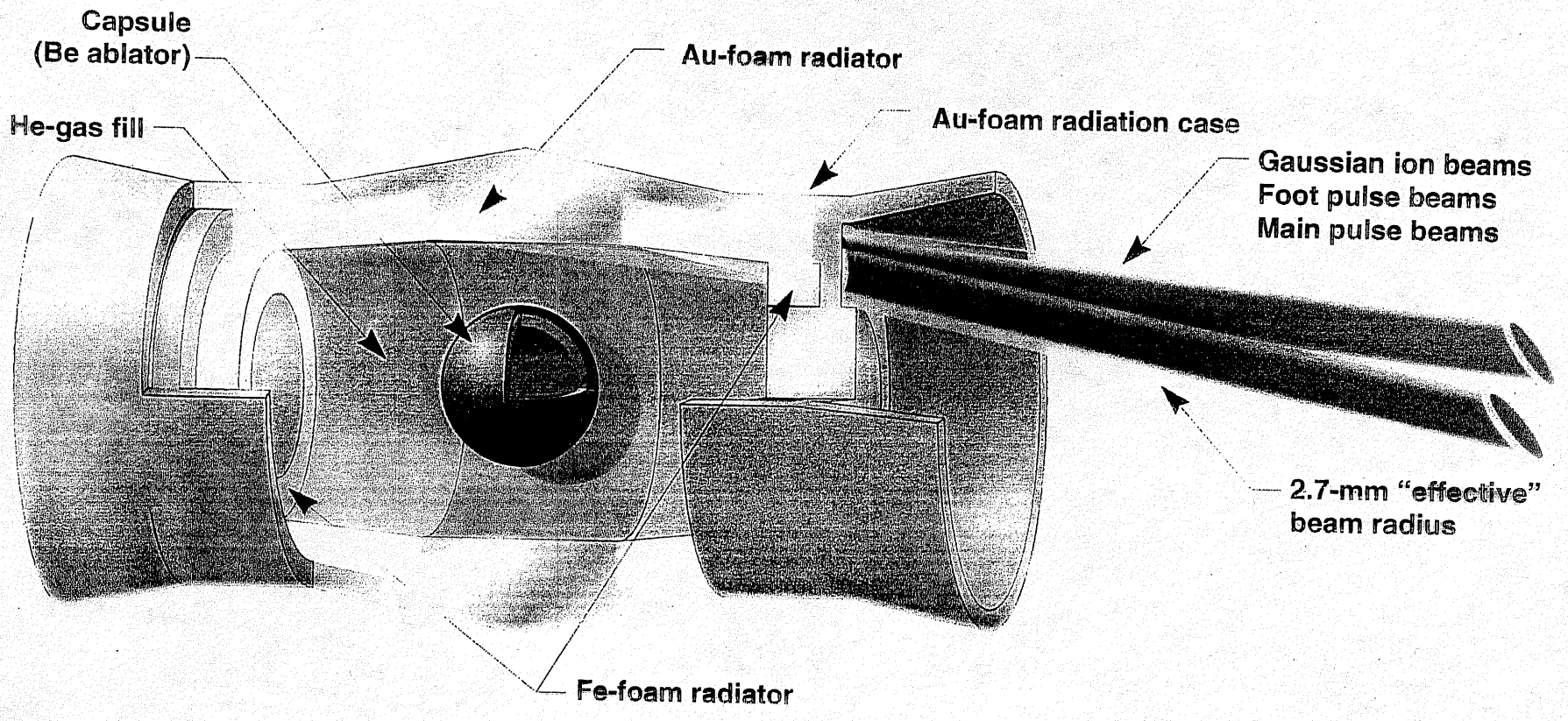

05-00-0998-1862A
9JDL/cld

9/10/98

The two principal approaches to ICF are direct drive and indirect drive

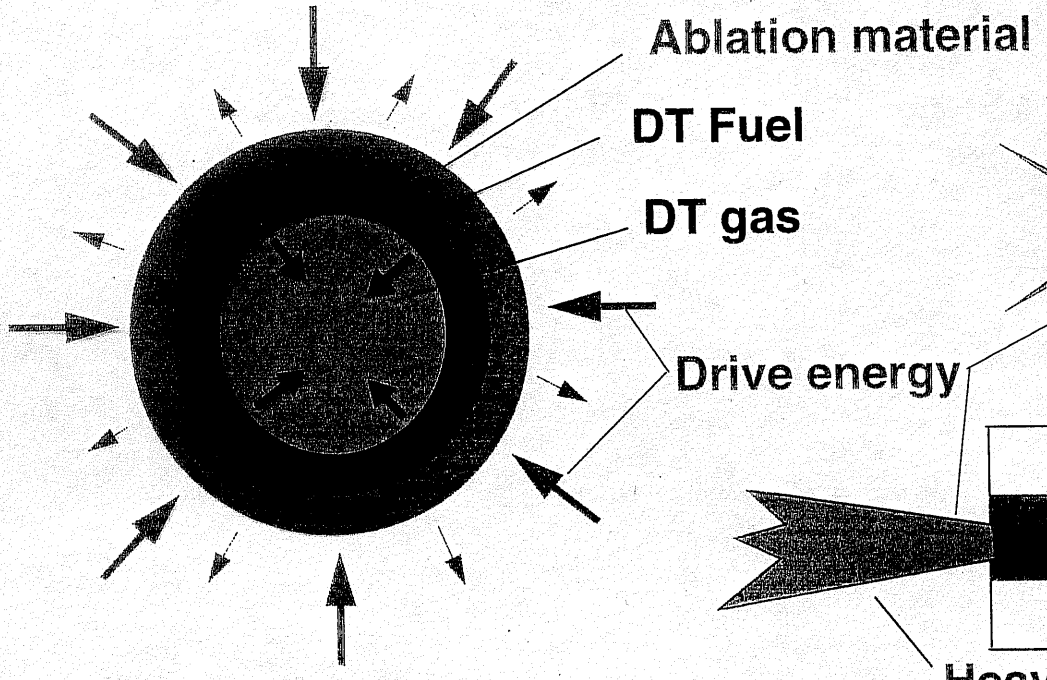

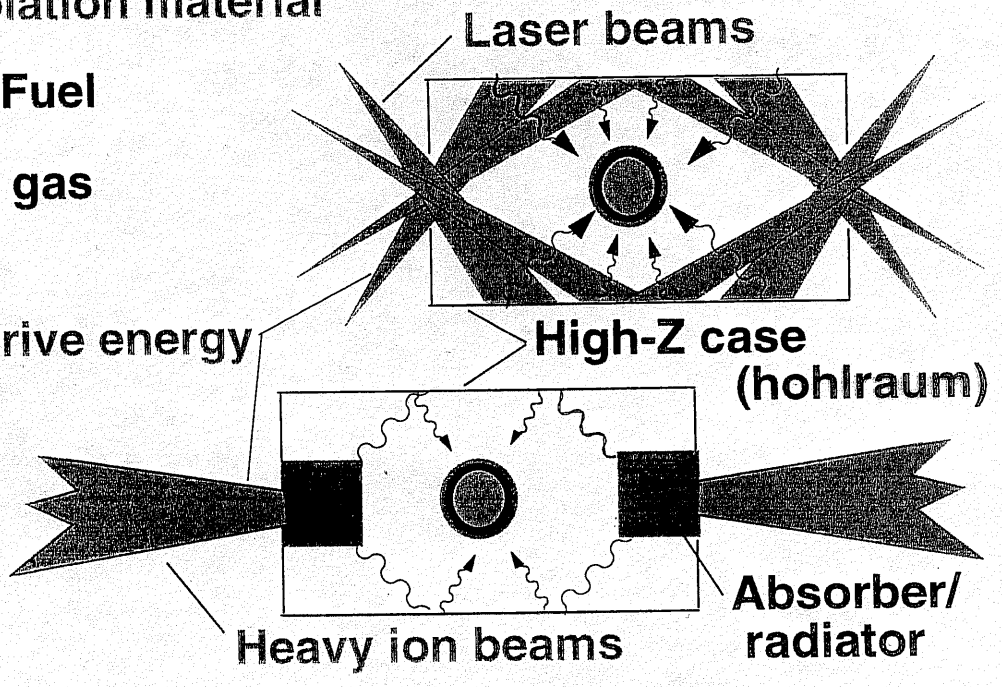

Direct drive:

Advantage:

- Higher coupling efficiency (with potential for higher gain)

Indirect drive:

Advantages:

- Relaxed beam uniformity (reduced hydro instability)
- Significant commonality for lasers and ion beams
- Significant simplification of chamber geometry

National Ignition Facility has 192 beams of 40-cm aperture arranged in four beam clusters

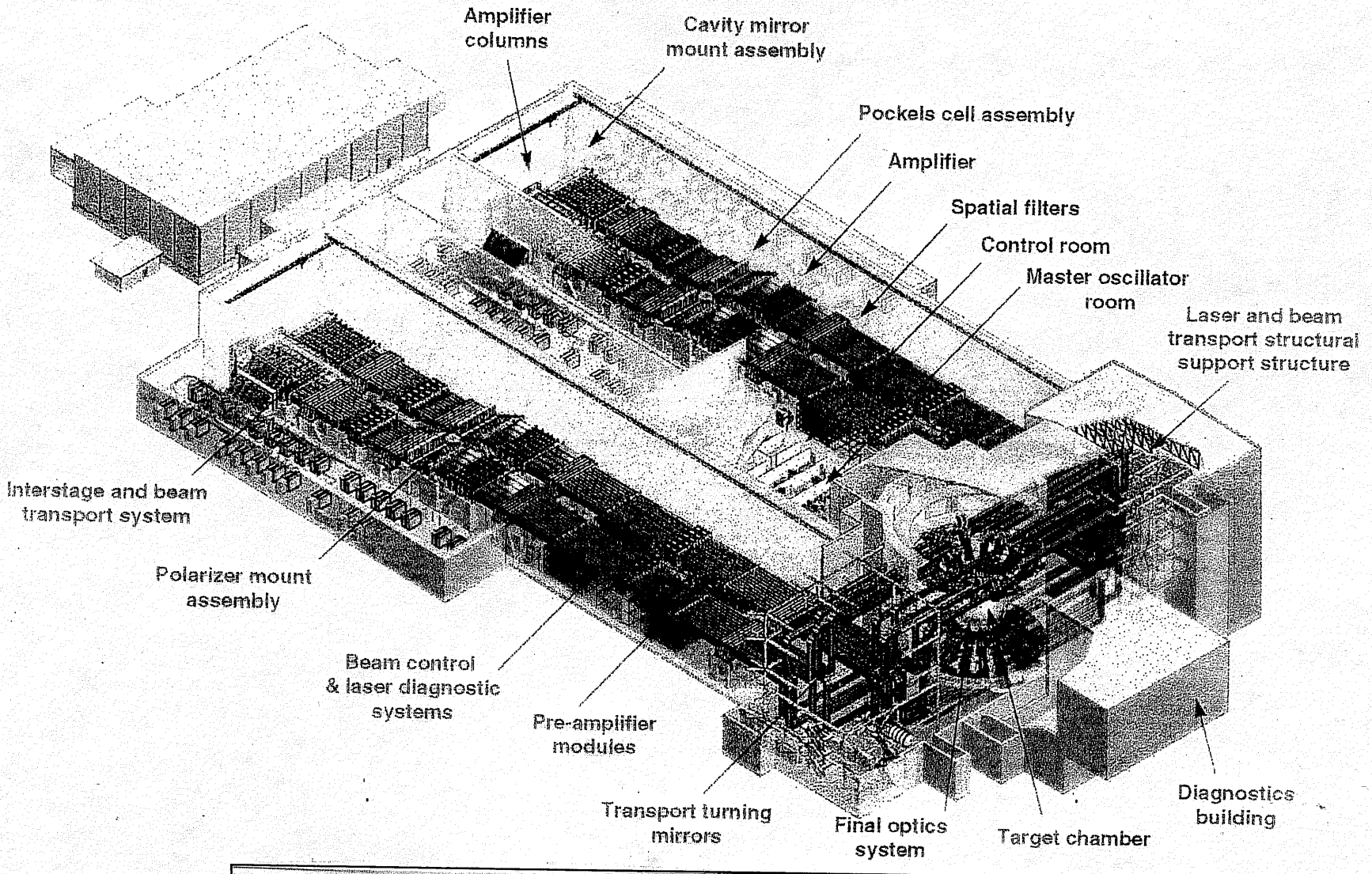

NIF illustrates many of the features of IFE development and will play a critical role in addressing IFE feasibility

40-00-0996-2100YA
03GAD/gbh

5/1/98
EMC/jco

2

Ion current profile and radiation temperature

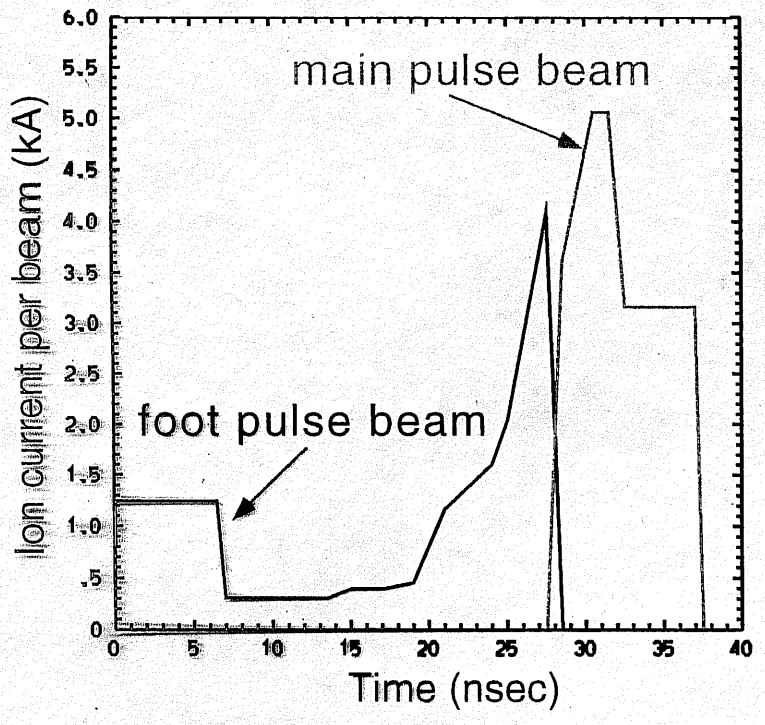

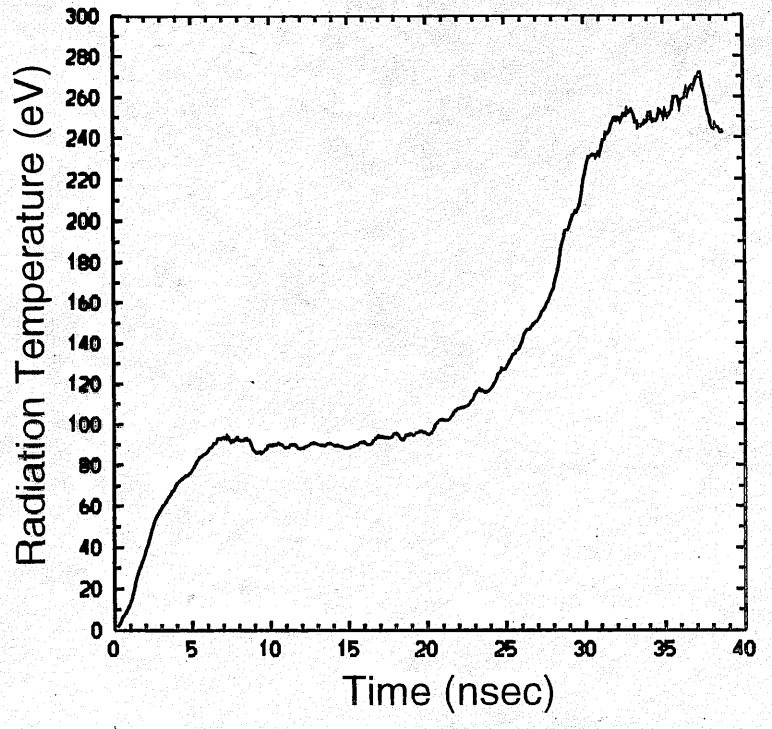

Current assumes 16 beams in foot pulse
32 beams in main pulse

Callahan 11/97

Overlapping Gaussian, elliptical beams are focused at the end of the target

Each beam is an ellipse

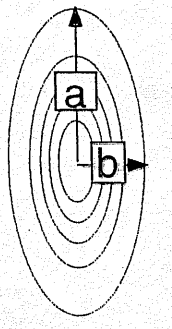

8 beams overlap in the foot pulse

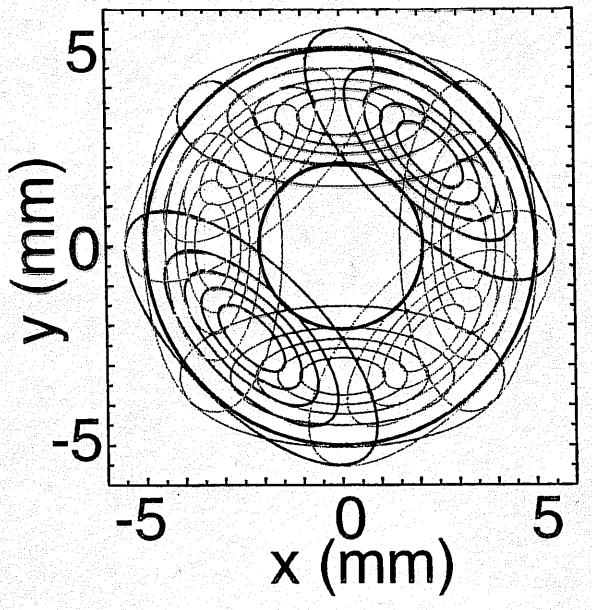

Sum of 8 foot pulse beams

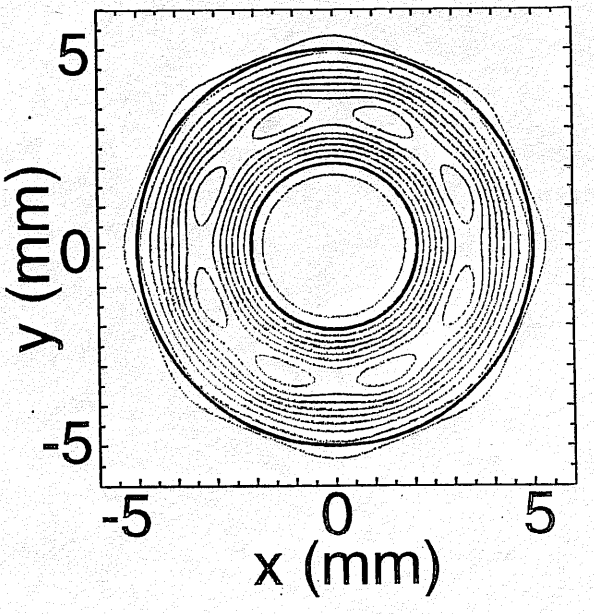

a = 4.15 mm
b = 1.8 mm
effective r=2.7 mm
95% of charge inside

Azimuthal asymmetry:
foot pulse: -1.6% in m=8
main pulse: 0.06% in m=16

Callahan 8/97

Why Heavy Ions?

Target requires:

3.5 - 6 MJ in ~ 10 ns ⇒ ~ 500 TW

Range ~ 0.02 - .2 g/cm²

Range requirement → **Higher mass ⇔ higher kinetic energy**

Power Requirement → **Current ∝ $\frac{1}{\text{kinetic energy}}$**

Higher mass requires lower current (easier to focus).

10

Heavier Ions ⇒ Higher Kinetic Energy

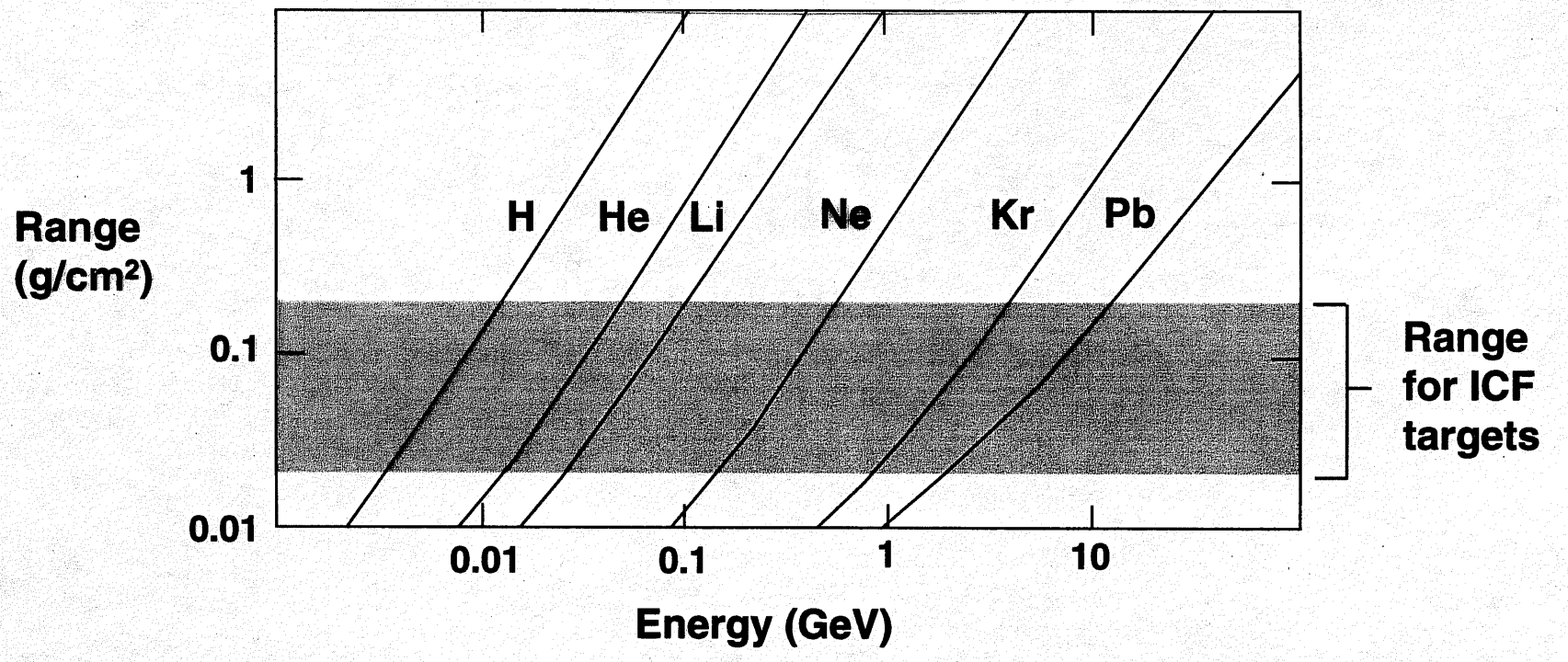

Targets require high power (kinetic energy x current).

- **Light Ion Fusion requires high-current, unconventional accelerators (Sandia 1970s).**
- **Heavy Ion Fusion requires lower currents enabling the use of more conventional high energy accelerators (Maschke ~ 1974).**

There are two principle methods of acceleration

1. r.f. acceleration

(Approach in Europe and Japan)

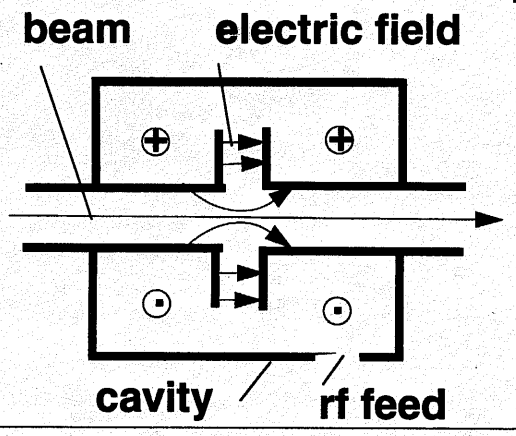

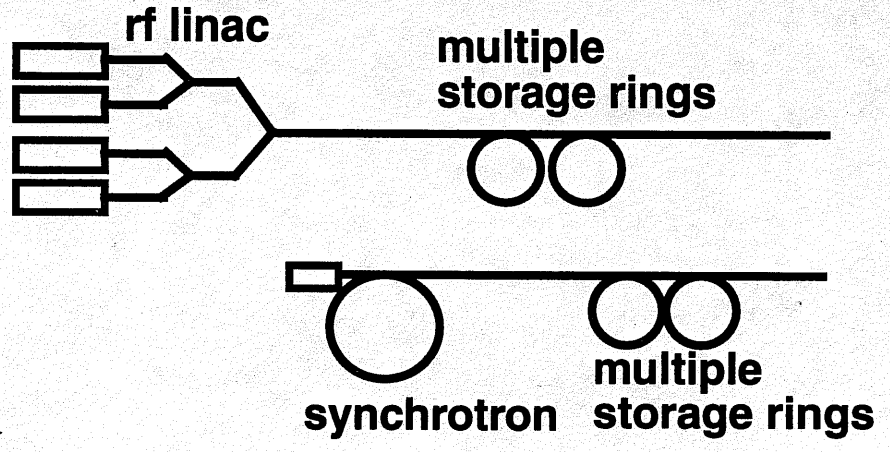

2. Induction acceleration

(U.S. approach)

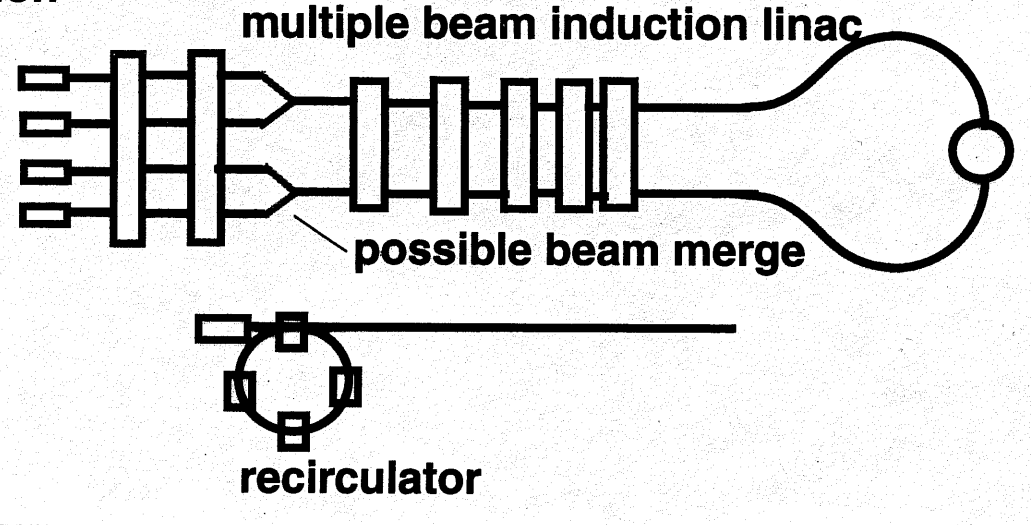

Induction acceleration for HIF consists of several subsystems and a variety of beam manipulations

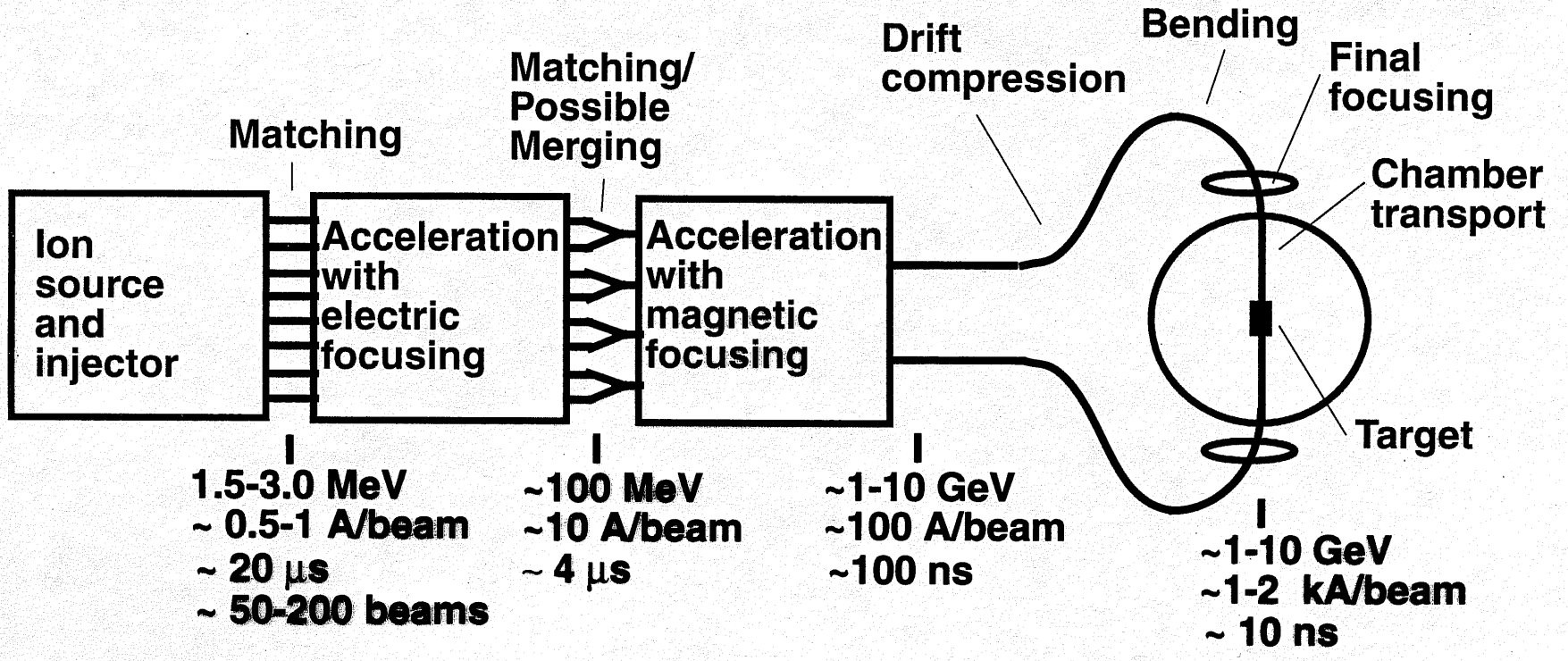

For "example IRE:"

1.6 MeV	9.4 MeV	200 MeV	200 MeV
0.8 A/beam	1.9 A/beam	15.3 A/beam	1.0 - 0.26 kA/beam
6.7 μs	2.8 μs	335 ns	5-20 ns
32 beams			

A Robust Point Design study established a baseline for a multiple-beam quadrupole induction linac HIF driver

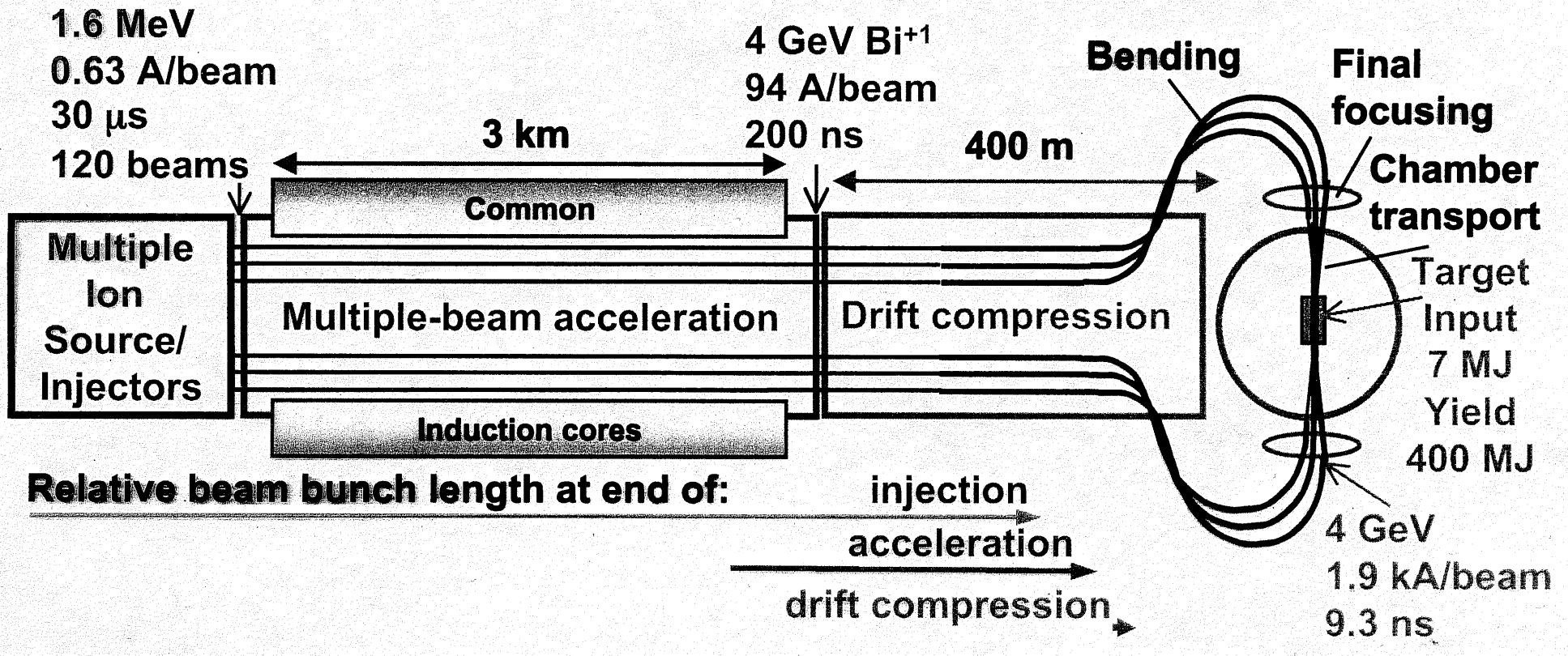

Major components of an induction linac

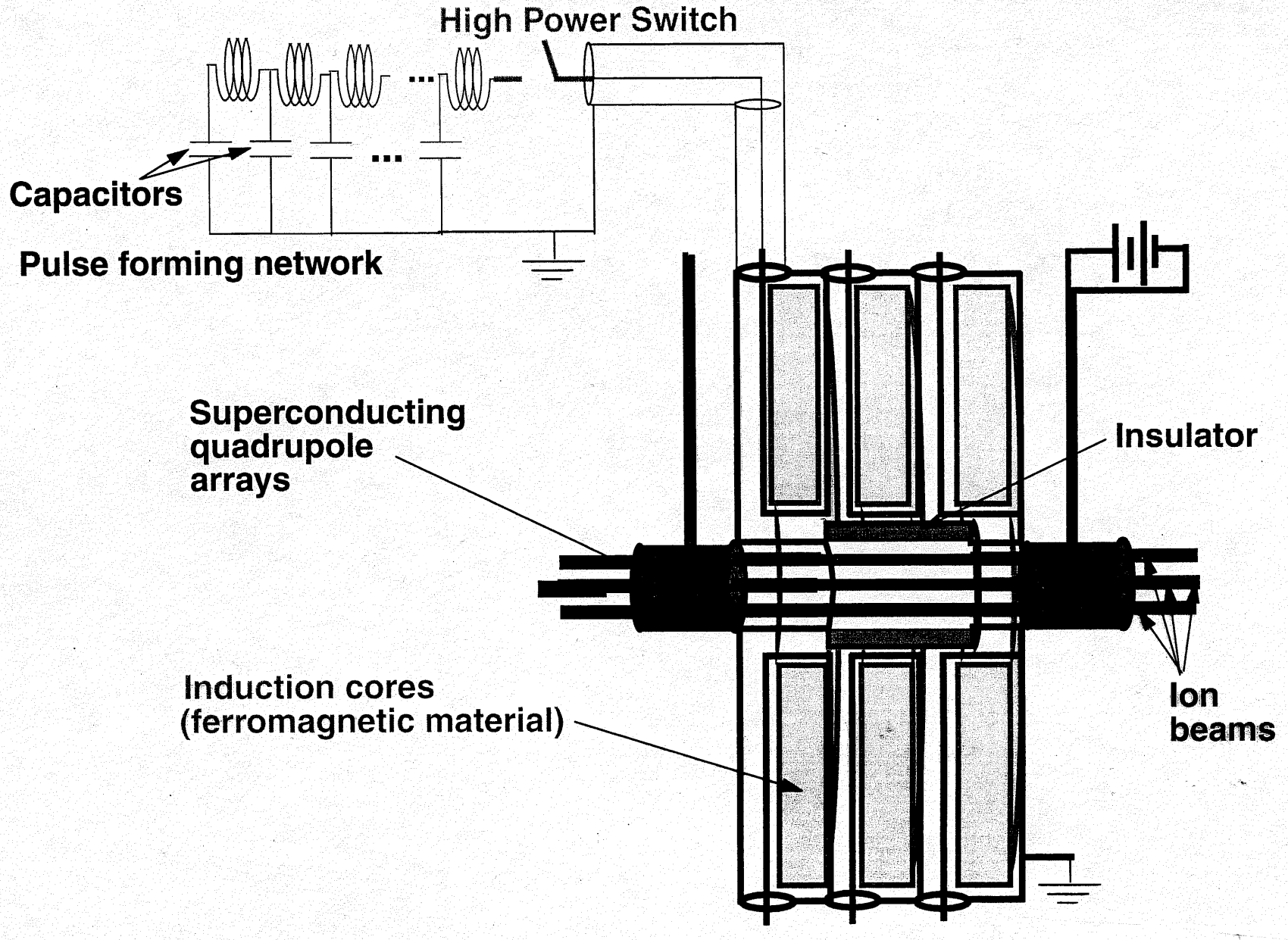

Induction acceleration: Cores and modulators

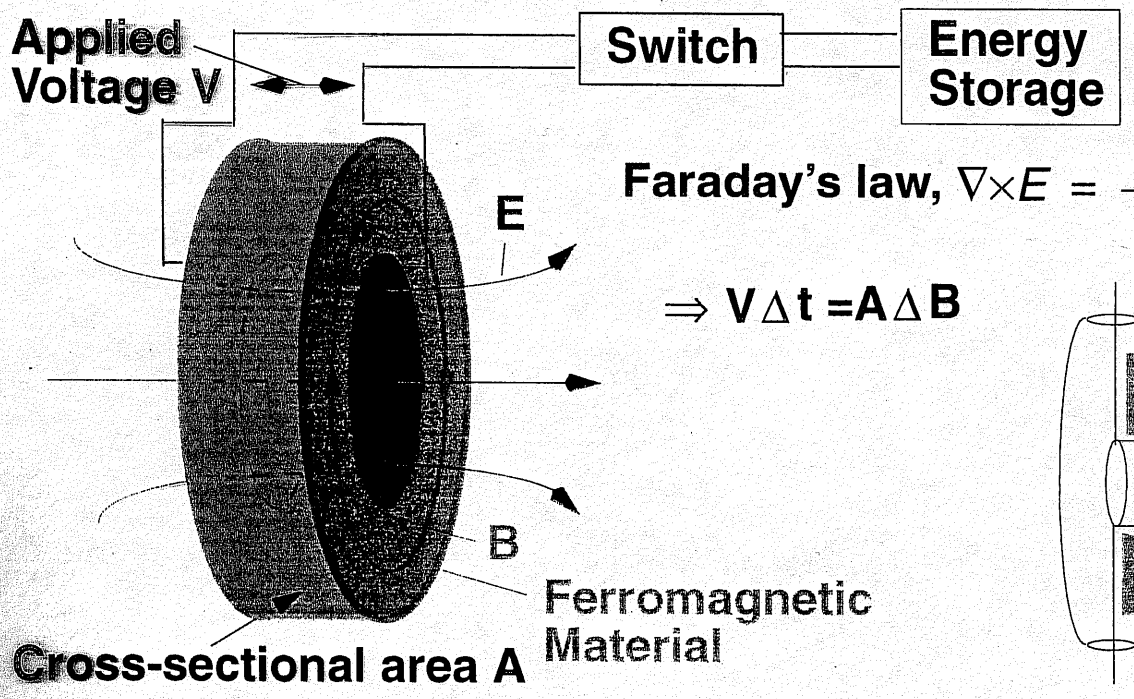

Faraday's law, $\nabla \times E = -\frac{\partial B}{\partial t}$

$\Rightarrow V \Delta t = A \Delta B$

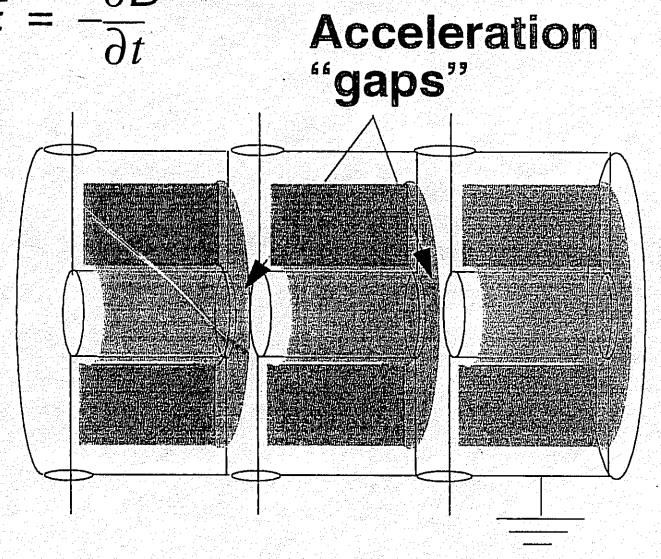

Different modulators used for linacs and recirculators:

Pulse forming network provides inexpensive, reproducible voltage pulse

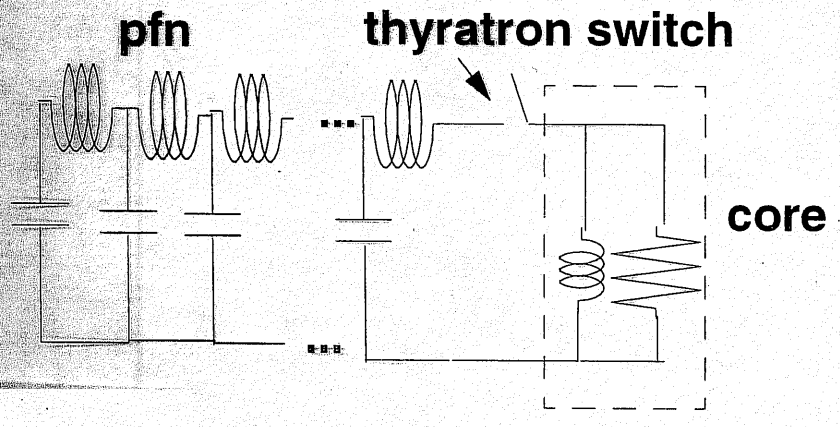

FET switches provide closing and opening capabilites for flexibility needed in recirculator

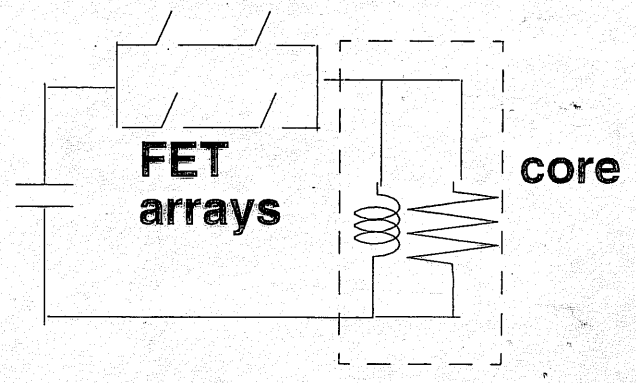

An Induction Core

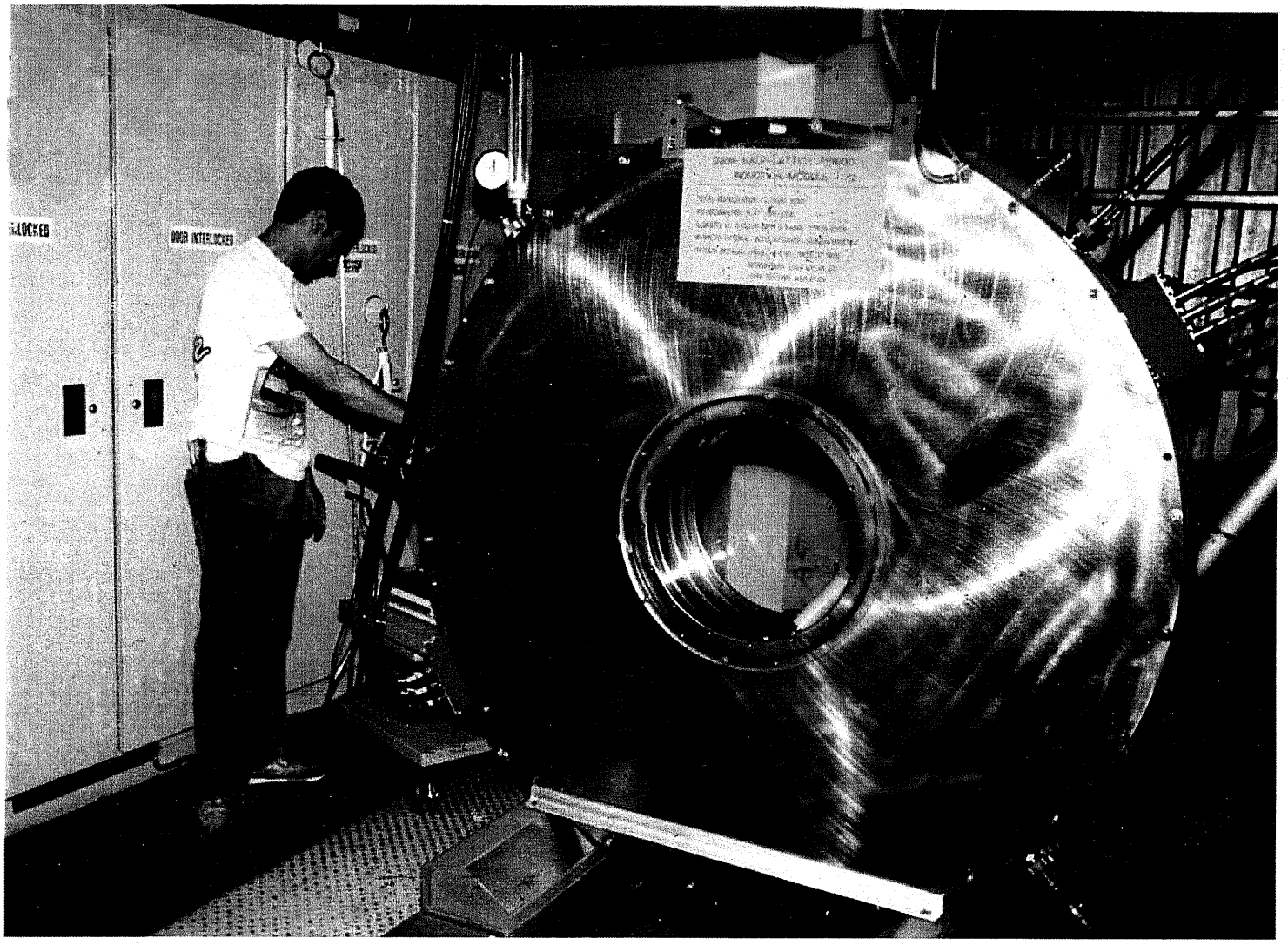

An array of small beamlets increases the total beam current through the core

From class:

$$\frac{Q}{a} = \left(\frac{a_0^2}{4l^2}\right) a_0$$

$$a_0 \cong \frac{4l^2}{(a_1)} \frac{B'}{}$$

$$I \sim \beta^3 Q$$

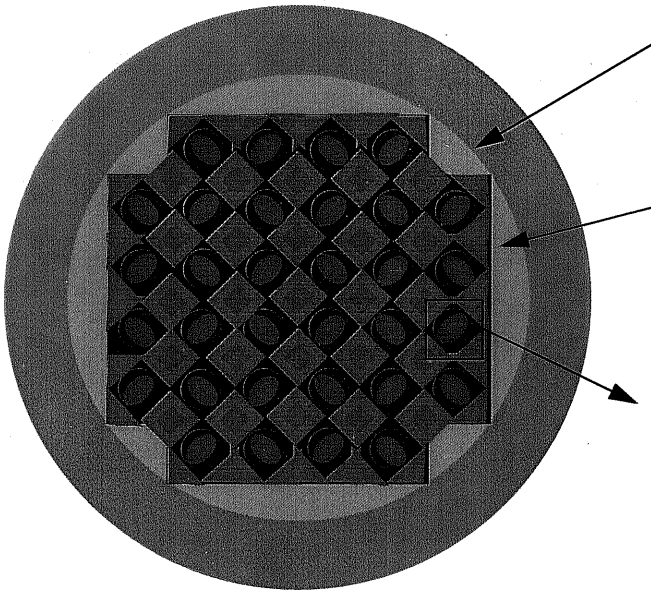

Core (radius = R_{core})

Multibeam quad array

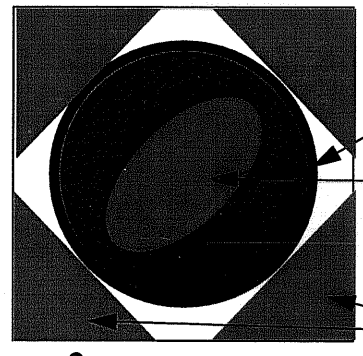

beam pipe (radius = r_p)

beam (radius = a)

quadrupole magnet winding

Current per beam = $I_b \sim a^2 B \beta^2/r_p$

$r_p \sim a$ (until misalignments require minimum size--better: $r_p = c_1 a + c_2$)

so $I_b \sim a$; N_b = number of beams in array $\sim R^2_{core} / a^2$

Total current through core = $I_{tot} = N_b I_b \sim R^2_{core} / a$ (until misalignments dominate scaling)

A Typical driver has about 2000 individual modules

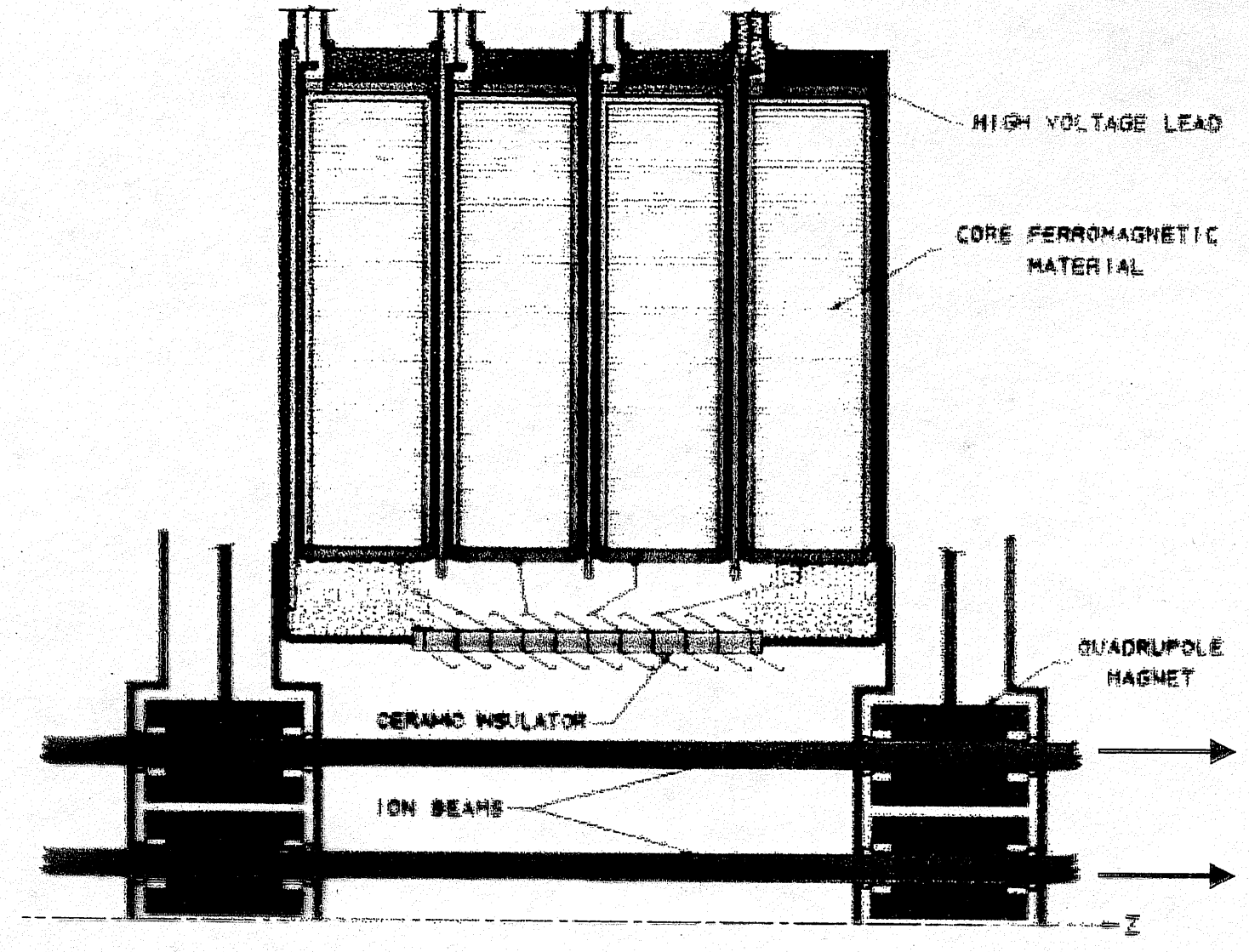

In an induction linac, certain limits constrain design

Phase advance per lattice period $\sigma_0 < \sim 85^\circ$ **(to avoid envelope/lattice instabilities} & emittance growth).**

Space charge is limited by external focusing $K < (\sigma_0 a/2L)^2$ **where K is the perveance (proportional to line charge density over beam Voltage), a is the average beam radius and L is the half-lattice period.**

Velocity tilt $\Delta v/v < \sim$ 0.3 for electrostatic quads **(larger for magnetic quads) to avoid mismatches at head and tail of beam, and to ensure tail radius within pipe and head σ_0 within limit)**

Volt-seconds per meter $(dV/ds)\, l/v_0$ <~ 1.5-2.0 V-s/m **(for "reasonable" core sizes)**

Voltage gradient dV/ds < ~ 1-2 MV/m **(to avoid breakdown in gaps)**

M. de Hoon studied a final current pulse that is flat with parabolic ends using the HERMES code

15 ns final pulse duration

The initial tilt on the beam is about 4% (compare to ~30% at the beginning of the accelerator)

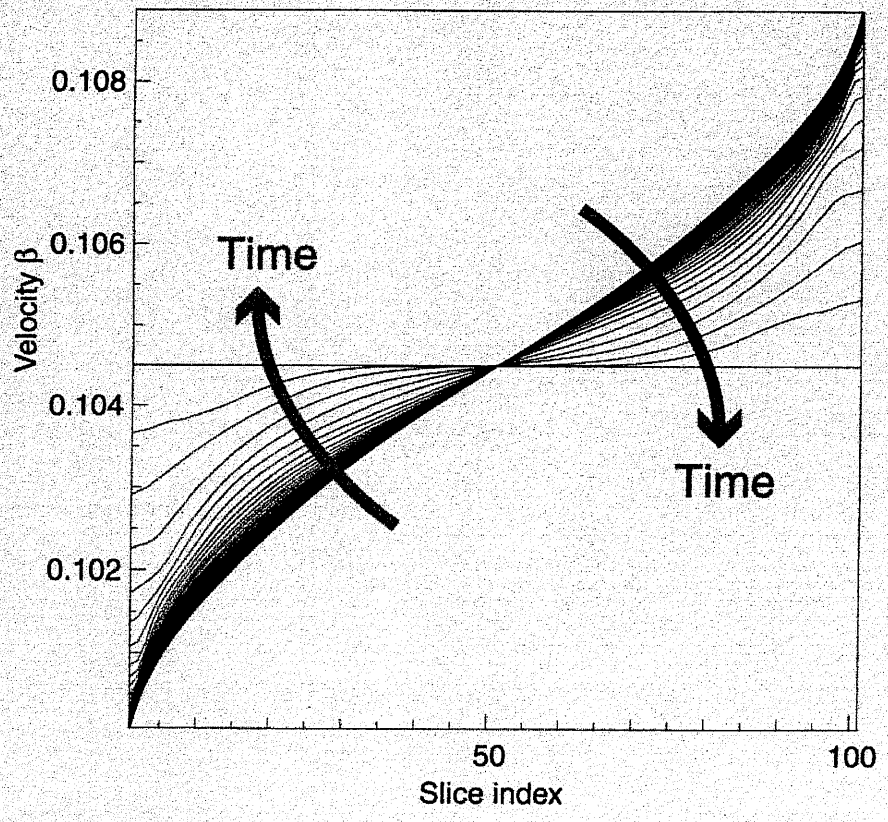

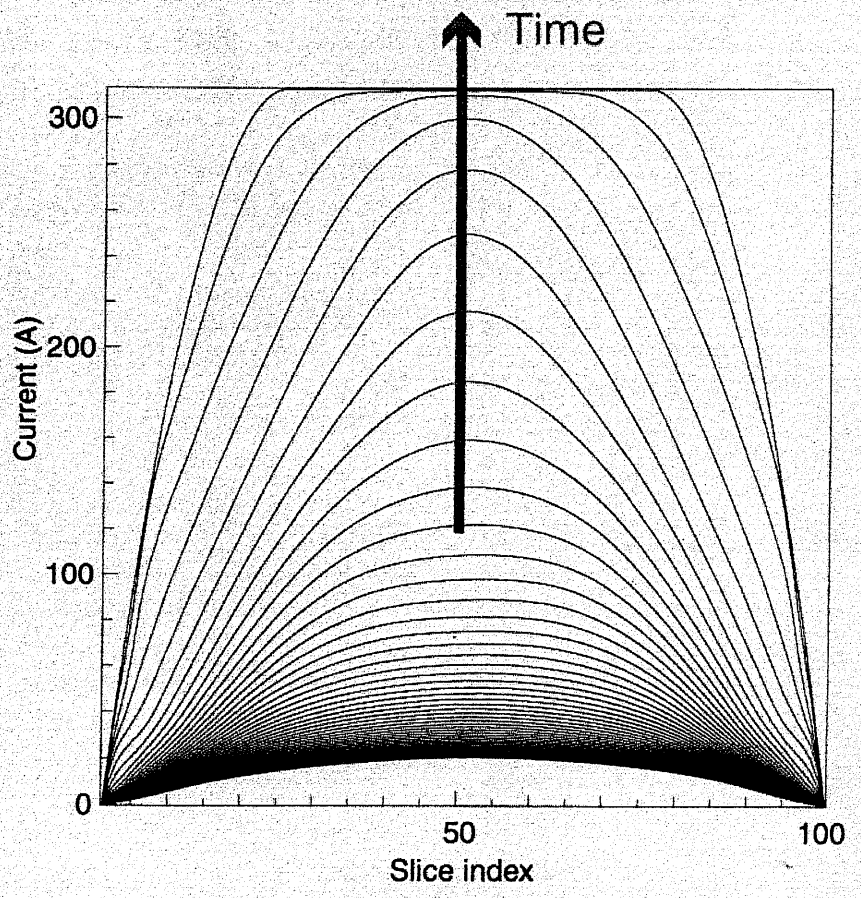

Although the final beam profile is flat, it is parabolic for most of the drift compression

Drift compression section is designed by running code first backwards from target, then forwards after rematching

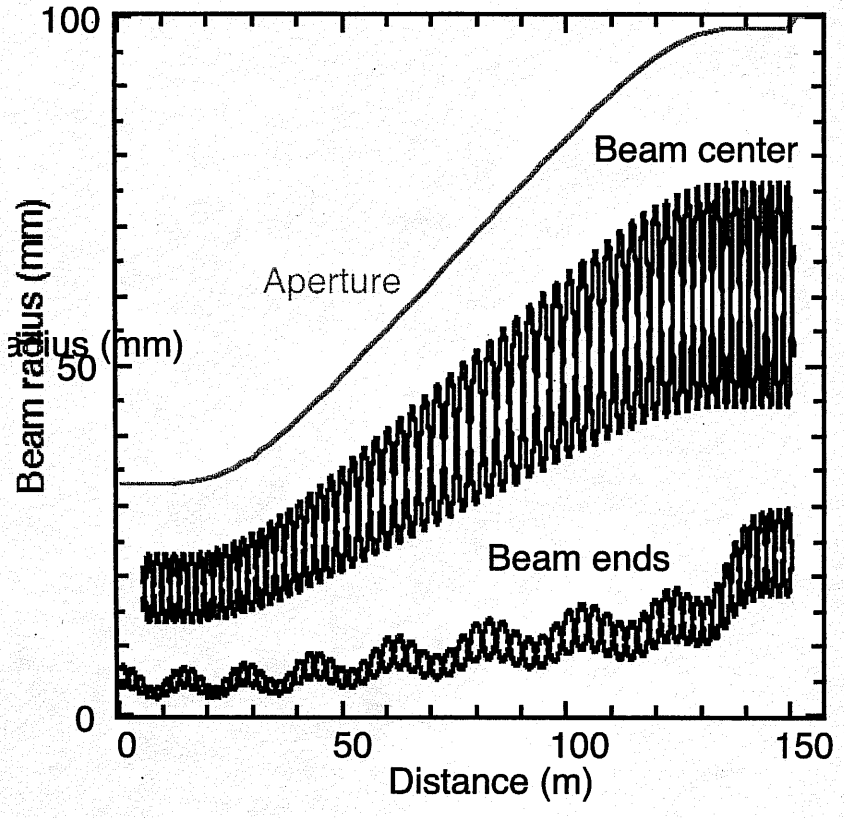

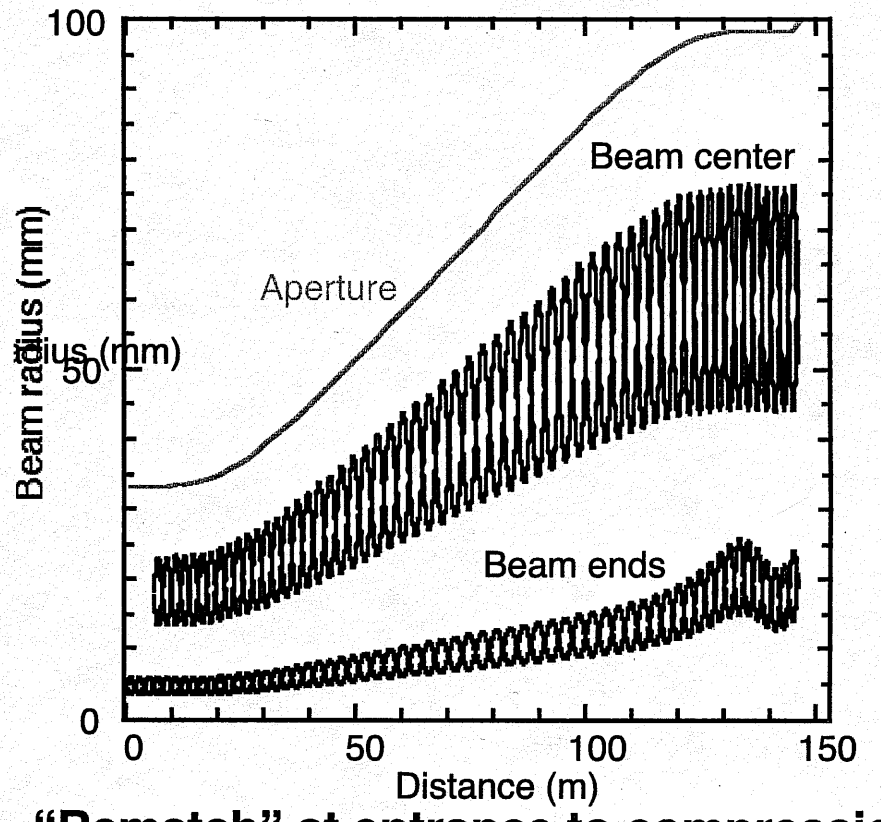

Begin with a desired 20ns, constant-energy pulse at end of compression, track backwards, design lattice for central slice; beam end becomes mismatched early on

"Rematch" at entrance to compression section, by adjusting a,a',b,b'; then track forward

Sources of non-linearity and mismatch are well defined

Sources of non-linearities

- External focusing magnets
- Space-charge
- Multiple-beam effects

Sources of mismatch

- Accelerator imperfections
  - Quad strength and placement errors
  - Acceleration waveform errors
  - Bend strength errors
- Velocity tilt

Simulations give reliable and definitive tolerances on each source

Several potential instabilities have been investigated in HIF drivers

Temperature anisotropy instability

After acceleration $T_{||} << T_{\perp}$, internal beam modes are unstable; saturation occurs when $T_{||} \sim T_{\perp}/3$

Longitudinal resistive instability

Module impedance interacts with beam, amplifying space-charge waves that are backward propagating in beam frame

Beam break-up (BBU) instability

High frequency waves in induction module cavities interact transversely with beam

Beam-plasma instability

Beam interacts with residual gas in target chamber

All of these instabilities have known analytic linear growth rates, which constrain the accelerator design (to ensure minimal growth or benign saturation).

A solenoid focus option leads to a low V, high current modular driver with advantageous development path

Pulse energy ~ 6.7 MJ

V~ 200-300 MV: T~ 2.5 GeV Xe^{+8} ions or T ~ 200 MeV for Ne^{+1}

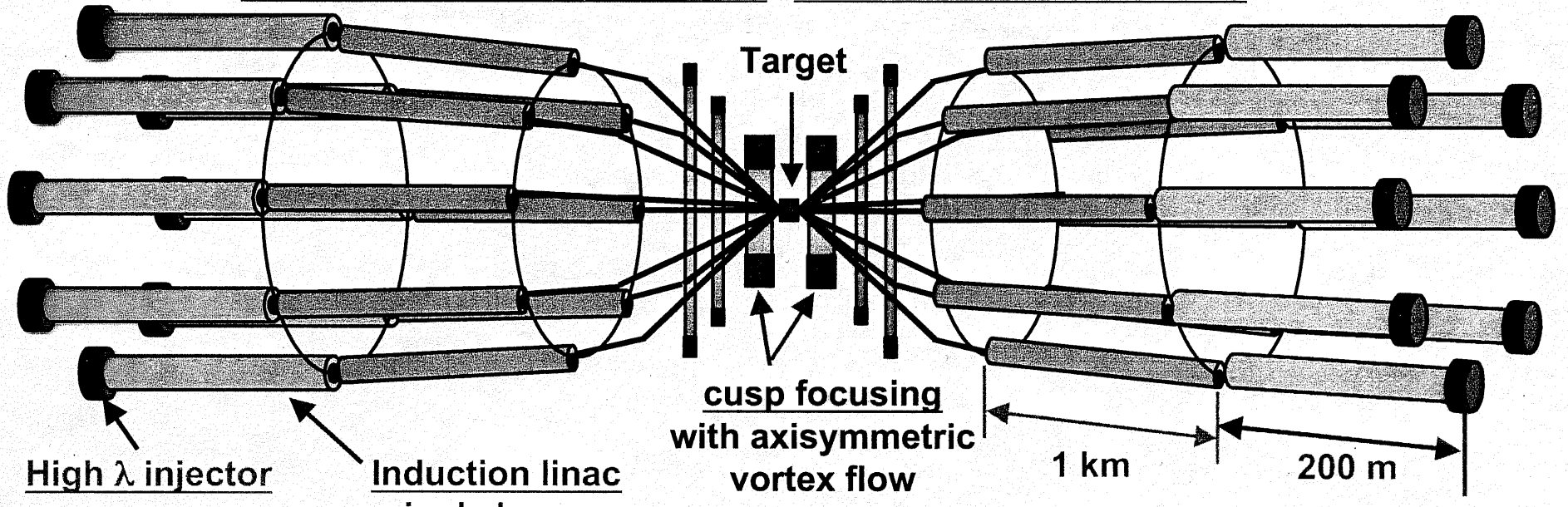

High λ injector

Merging beamlet source/injector

or

accel/decel injector

Induction linac

single beams

r_p ~ 15 cm

B_s ~ 9T

I ~ 6.7 kA

T ~ 2.5 GeV

Δt ~ 100 ns

double pulsed for foot and main pulses

cusp focusing with axisymmetric vortex flow

or

adiabatic plasma lense assisted pinch with cross-jet flow. liquid walls

Neutralized drift compression

Δv/v ~ 0.01

(no space charge stagnation)

Integration of target,chamber, and accelerator requirements led to the self-consistent point design

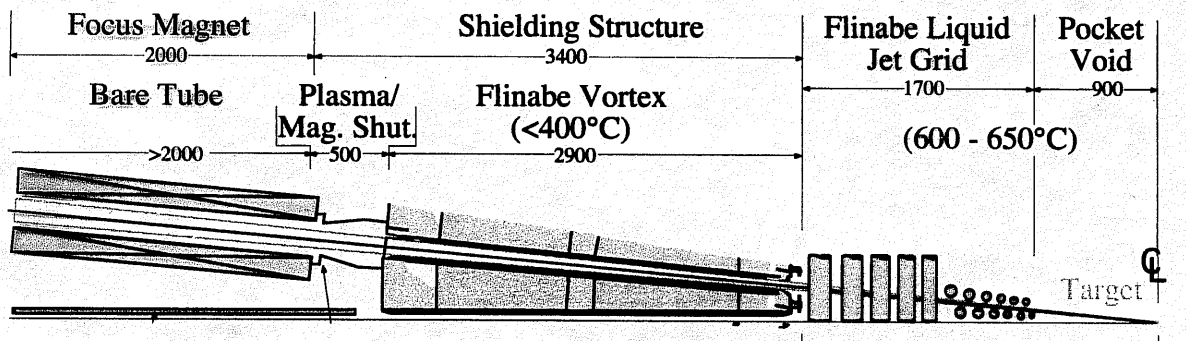

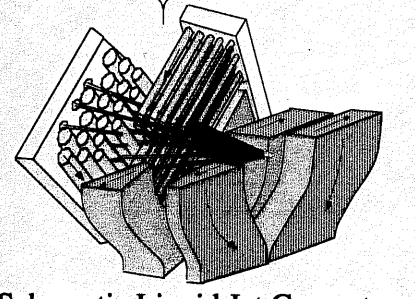

Schematic Liquid Jet Geometry

Chamber dynamics

Ion: Bi^+ (A=209)
Main pulse: 4 GeV
Foot pulse: 3.3 GeV
120 beams total (72 main, 48 foot)
Pulse energy: 7 MJ
Final spot radius: 2.2 mm

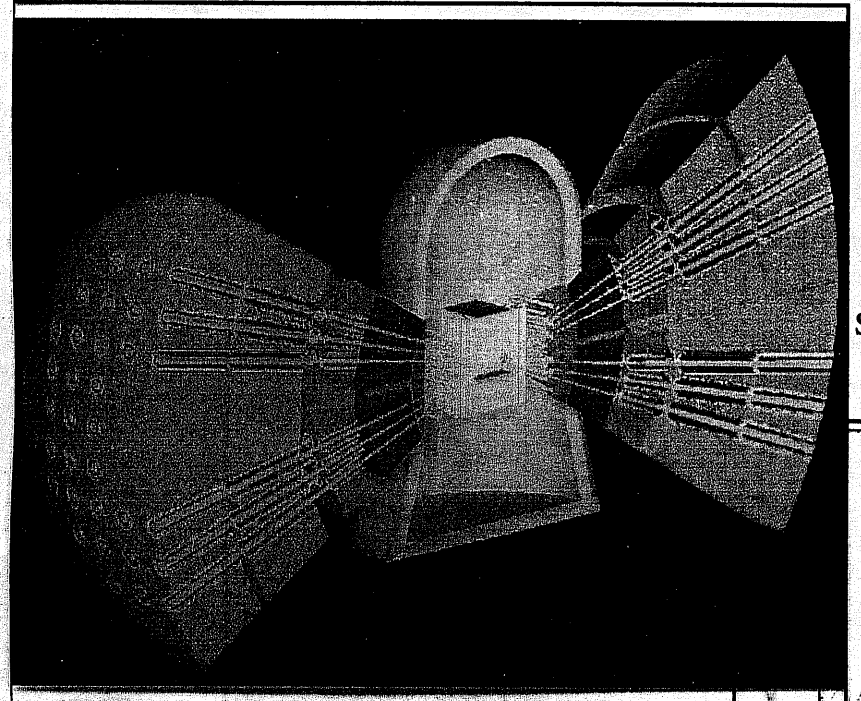

3 D neutronics calculations

Length: 2.7 km; Efficiency 28%
Total cost: 2.8 B$

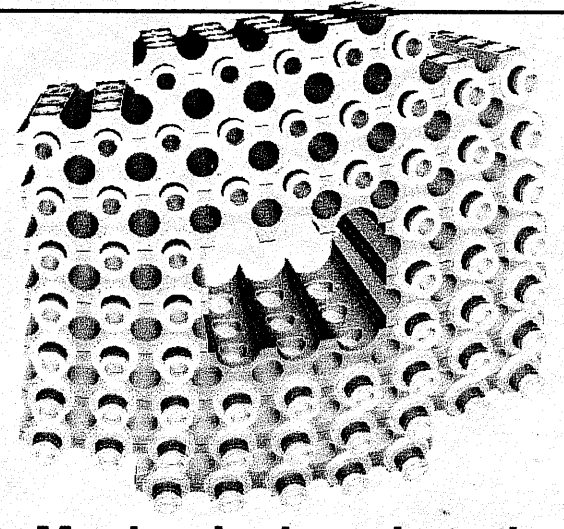

Mechanical engineering

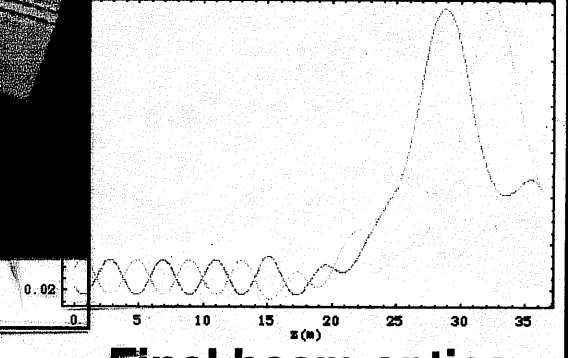

Final beam optics

+ target physics + chamber propagation

The HYLIFE-II Ion beam-driven power plant is shown with a two-end target, illustrated from two sides and a linear heavy-ion induction driver

The liquid wall protection including beam ports is provided by pumping molten salt (Flibe) through the chamber

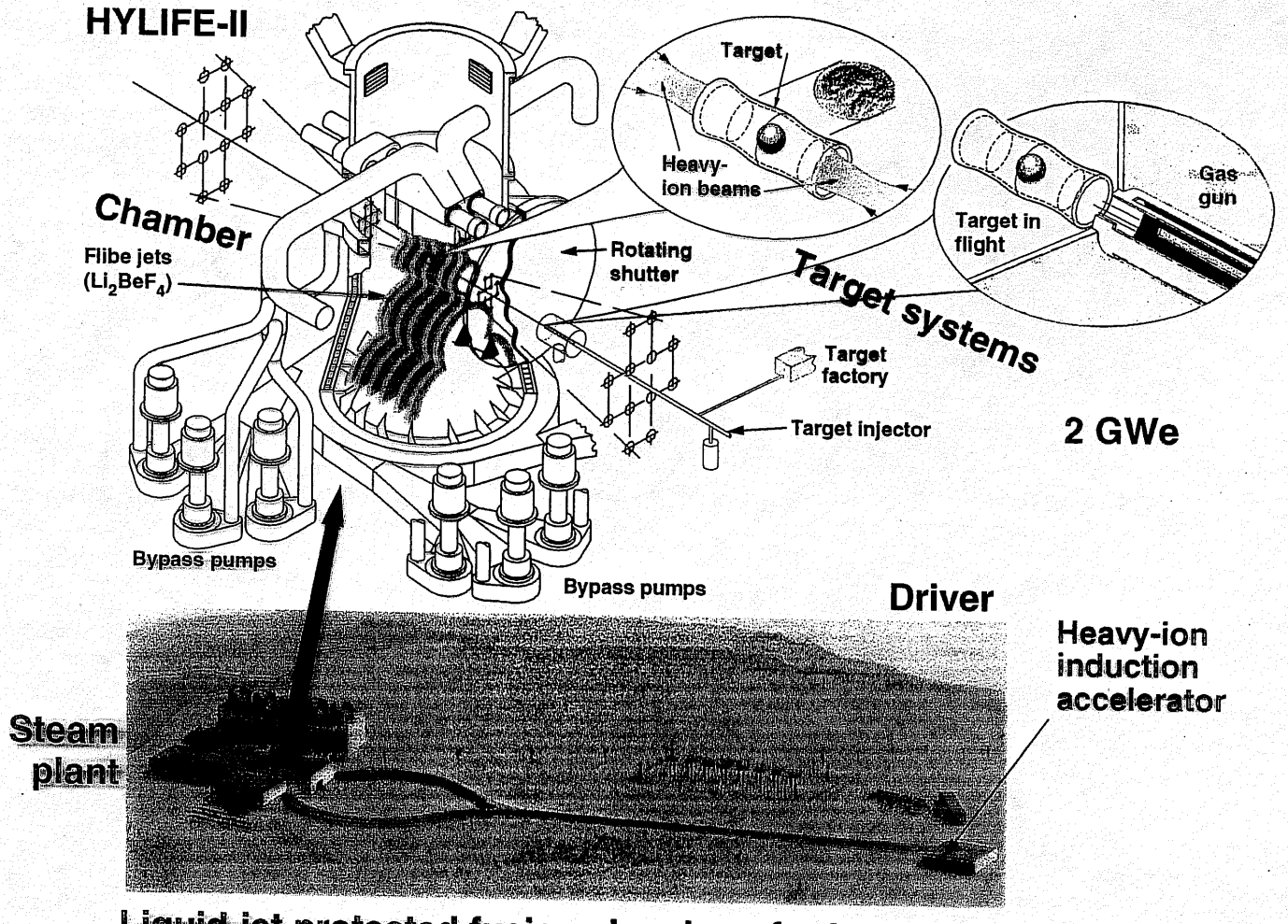

Liquid-jet protected fusion chambers for long lifetime, low cost, and low environmental impact

05-00-1194-3846U
16RWM/gbh

10/7/98

A number of final focus options are being considered for HIF applications

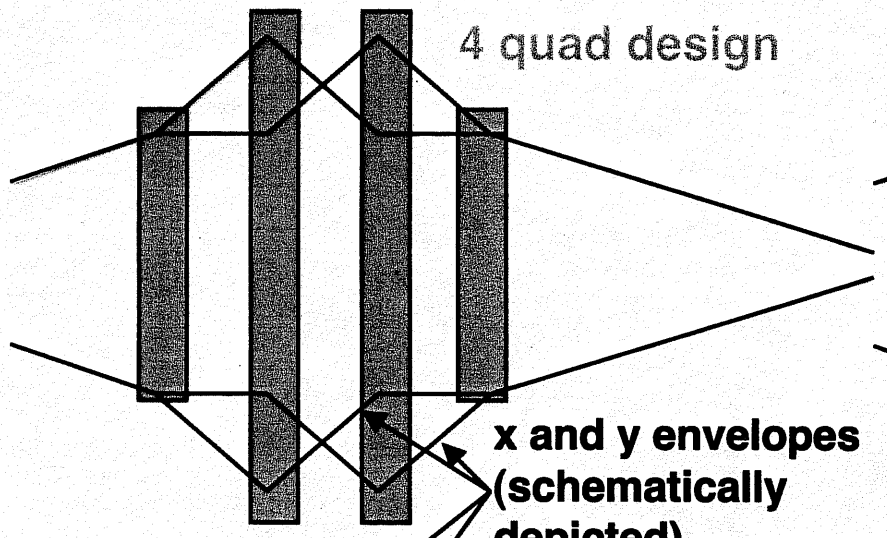

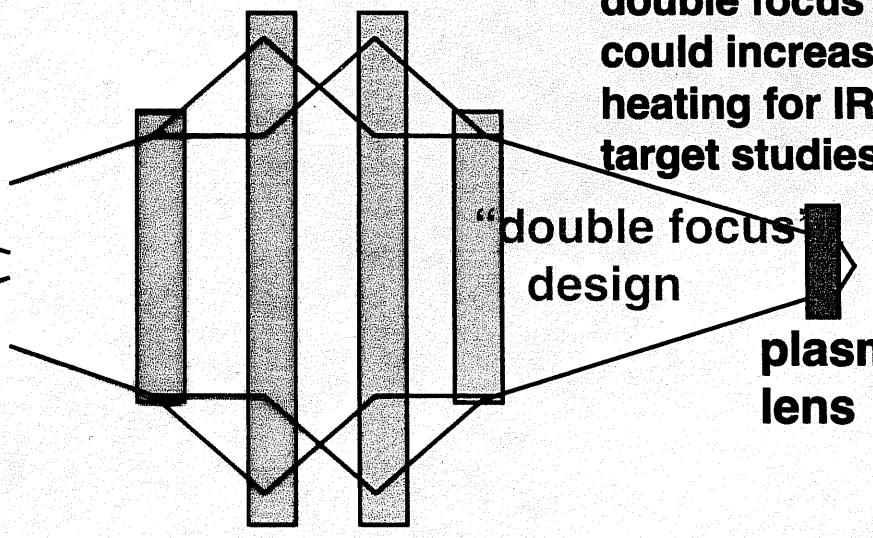

double focus design could increase spot heating for IRE target studies

x and y envelopes (schematically depicted)

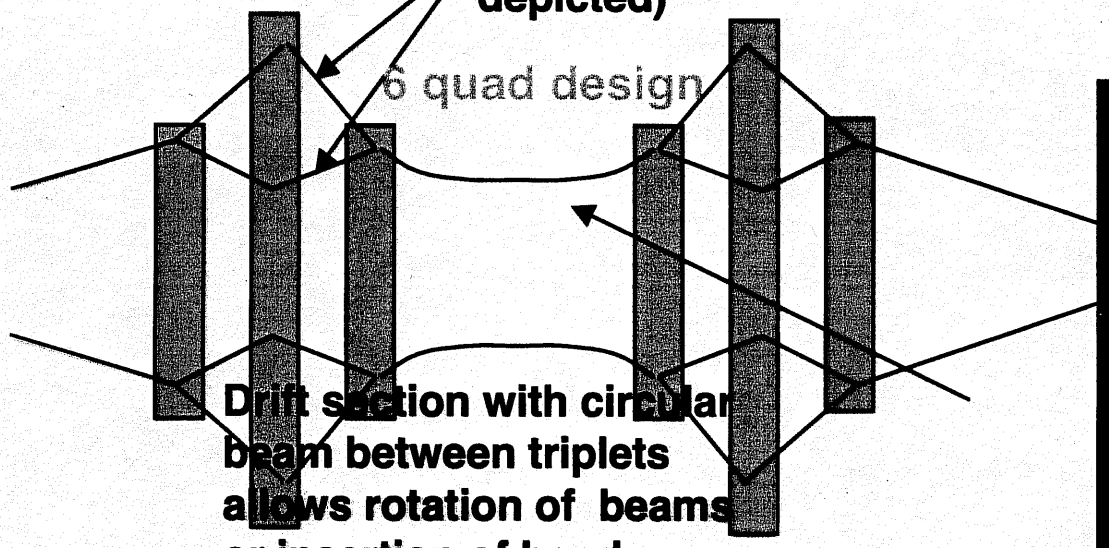

Drift section with circular beam between triplets allows rotation of beams or insertion of bend

Solenoid or cusp focusing is being considered for modular drivers:

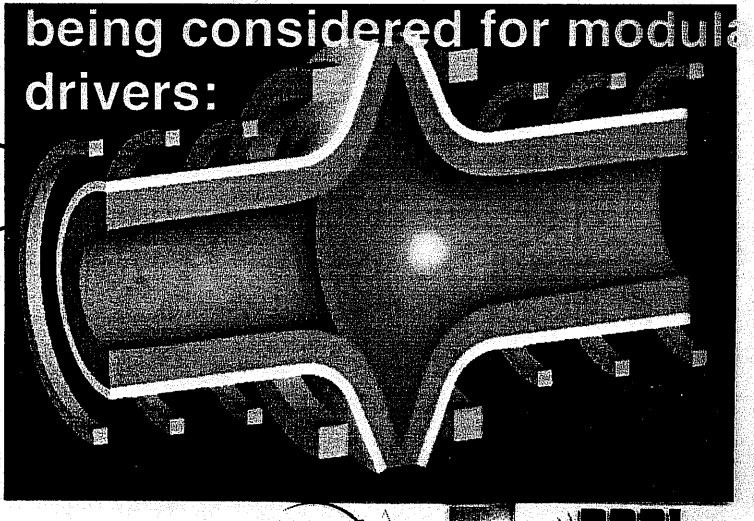

A range in ion velocities, implies a range in focal lengths, and a focal spot radius which is larger than the emittance-limited radius

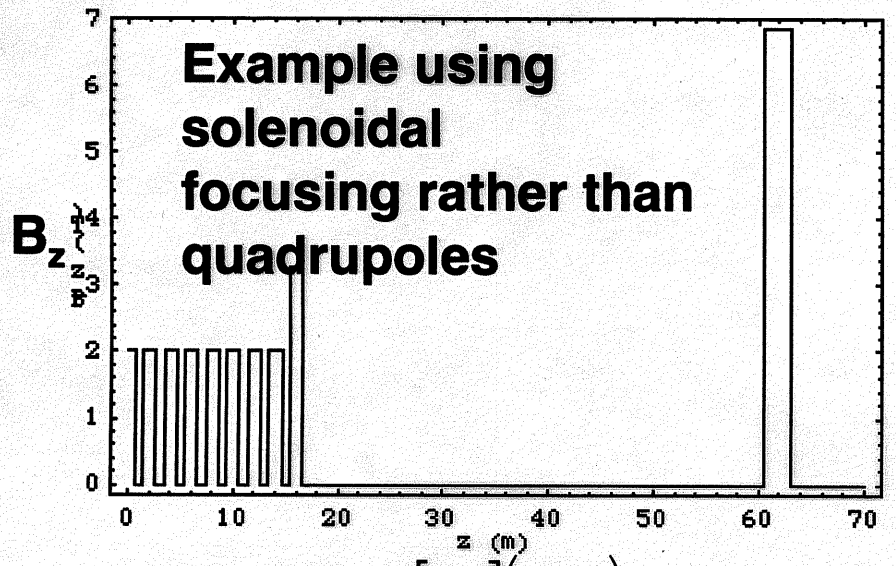

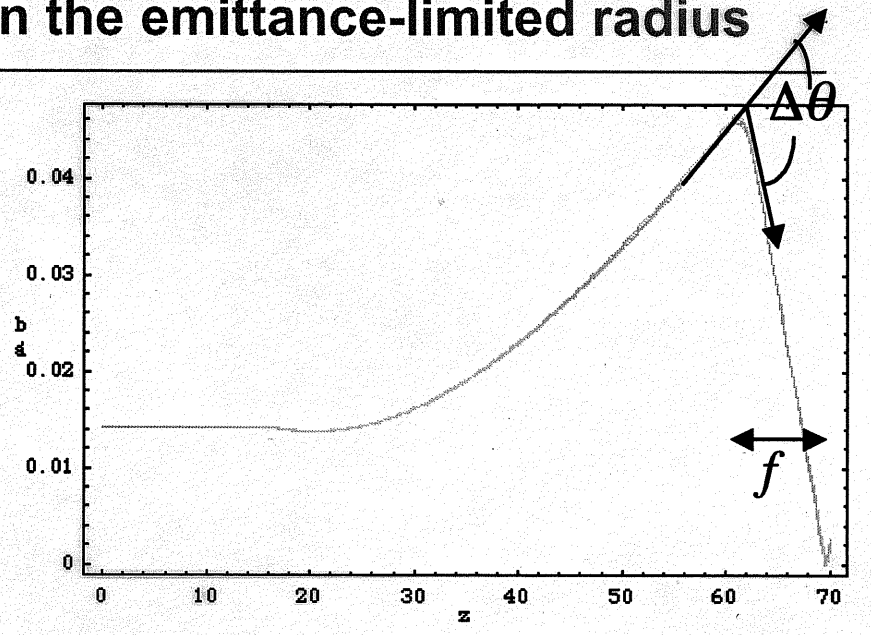

$$r_{spot} = \theta\,\delta f = \theta\left[\frac{df}{d\theta}\right]\left(\frac{d\Delta\theta}{dp}\right)\delta p$$

$$= \theta\left[\frac{f}{\theta}\right]\left(\frac{2\Delta\theta}{p}\right)\delta p$$

$$r_{spot} \cong 2 f \Delta\theta(\delta p / p)$$

For "point-to-point" focus $\Delta\theta = 2\theta$

$$r_{spot} \cong 4 f \theta(\delta p / p)$$

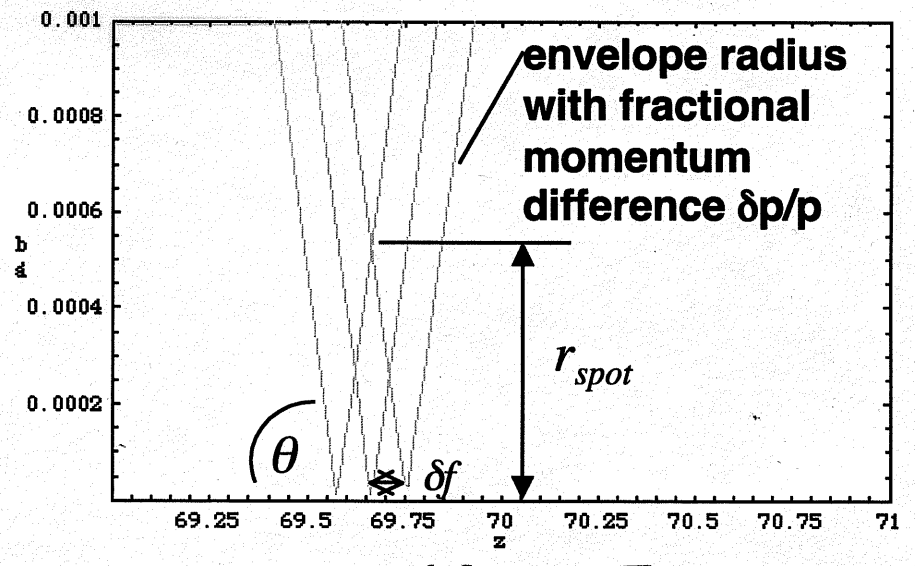

We constructed moment models to study chromatic effects (through 2nd order) in final focus system

$$\frac{dp_x}{dt} = q(E_x + v_z B_y - v_y B_z)$$

Expand through 2nd order in x', y', $k_{\beta 0}x$, $k_{\beta 0}y$, $\delta p/p$

$$x'' + \left(\frac{1}{\gamma v_{z0}}\frac{d}{dz}(\gamma v_z)\right)x' \cong \frac{qB'}{\gamma m v_{z0}}x\left(1 - \frac{\delta p}{p}\right) + \frac{q\lambda}{4\pi\varepsilon_0 m v_{z0}^2}\frac{(x-\bar{x})(1-\frac{2\delta p}{p})}{(\Delta x^2 + [\Delta x^2 \Delta y^2]^{1/2})}$$

The equation of motions can be written (where $\delta = \delta p/p$**) :**

$$\boxed{x'' \cong K_{xx}x + K_{xx1}x\delta \qquad y'' \cong K_{yy}y + K_{yy1}y\delta}$$

Here:

$$K_{xx} = \frac{B'}{[B\rho]_0} + \frac{Q}{2(\Delta x^2 + [\Delta x^2 \Delta y^2]^{1/2})} \qquad K_{yy} = \frac{-B'}{[B\rho]_0} + \frac{Q}{2(\Delta y^2 + [\Delta x^2 \Delta y^2]^{1/2})}$$

$$K_{xx1} = -\left[\frac{B'}{[B\rho]_0} + \frac{2Q}{2(\Delta x^2 + [\Delta x^2 \Delta y^2]^{1/2})}\right] \qquad K_{yy1} = -\left[\frac{-B'}{[B\rho]_0} + \frac{2Q}{2(\Delta y^2 + [\Delta x^2 \Delta y^2]^{1/2})}\right]$$

B' = **quadrupole gradient;** $[B\rho]$ = **Ion rigidity** $= p/q$; Q = **perveance** $= \frac{q\lambda}{2\pi\varepsilon_0 \gamma_0^3 m v_{z0}^2}$

We take averages of 2nd, 3rd,... order quantities, forming infinite set of 1st order ode's

$$\frac{d}{ds}\langle x^2\rangle = 2\langle xx'\rangle$$

$$\frac{d}{ds}\langle xx'\rangle = \langle x'^2\rangle + \langle xx''\rangle$$

$$= \langle x'^2\rangle + K_{xx}\langle x^2\rangle + \underline{K_{xx1}\langle x^2\delta\rangle}$$

$$\frac{d}{ds}\langle x'^2\rangle = 2\langle x'x''\rangle$$

$$= 2K_{xx}\langle xx'\rangle + \underline{2K_{xx1}\langle xx'\delta\rangle}$$

$$\frac{d}{ds}\langle x^2\delta\rangle = 2\langle xx'\delta\rangle$$

$$\frac{d}{ds}\langle xx'\delta\rangle = \langle x'^2\delta\rangle + \langle xx''\delta\rangle$$

$$= \langle x'^2\delta\rangle + K_{xx}\langle x^2\delta\rangle + \underline{K_{xx1}\langle x^2\delta^2\rangle}$$

$$\frac{d}{ds}\langle x'^2\delta\rangle = 2\langle x'x''\delta\rangle$$

$$= 2K_{xx}\langle xx'\delta\rangle + \underline{2K_{xx1}\langle xx'\delta^2\rangle}$$

...

$$\frac{d}{ds}\langle x^2\delta^n\rangle = 2\langle xx'\delta^n\rangle$$

$$\frac{d}{ds}\langle xx'\delta^n\rangle = \langle x'^2\delta^n\rangle + \langle xx''\delta^n\rangle$$

$$= \langle x'^2\delta^n\rangle + K_{xx}\langle x^2\delta^n\rangle + \underline{K_{xx1}\langle x^2\delta^{n+1}\rangle}$$

$$\frac{d}{ds}\langle x'^2\delta^n\rangle = 2\langle x'x''\delta^n\rangle$$

$$= 2K_{xx}\langle xx'\delta^n\rangle + \underline{2K_{xx1}\langle xx'\delta^{n+1}\rangle}$$

=> term higher order by one

Infinite set of equations can be truncated, but are reliable over only finite distances

Two equivalent methods of truncation have been employed:

1. $\langle x^2\delta^2\rangle \sim \langle x^2\rangle\langle\delta^2\rangle$ and $\langle xx'\delta^2\rangle \sim \langle xx'\rangle\langle\delta^2\rangle$; or
2. Noticing that $\frac{1}{1+\delta} = 1-\delta+\delta^2+\ldots$ and $\frac{1}{1-\delta} = 1+\delta+\delta^2+\ldots$ thus,

$$\frac{1}{1-\delta}-\frac{1}{1+\delta} = 2\delta+2\delta^3+\ldots \quad \text{also} \quad \frac{\delta}{1+\delta} = 1-\frac{1}{1+\delta}$$

so that we may, to good approximation, write

$$\frac{d}{ds}\langle x^2\rangle = 2\langle xx'\rangle \qquad \frac{d}{ds}\langle xx'\rangle = \langle x'^2\rangle + K_{xx}\langle x^2\rangle + \frac{K_{xx1}}{2}\left[\left\langle\frac{x^2}{1-\delta}\right\rangle - \left\langle\frac{x^2}{1+\delta}\right\rangle\right] + O\left(x^2\delta^3\right)$$

$$\frac{d}{ds}\langle x'^2\rangle = 2K_{xx}\langle xx'\rangle + K_{xx1}\left[\left\langle\frac{xx'}{1-\delta}\right\rangle - \left\langle\frac{xx'}{1+\delta}\right\rangle\right] + O(xx'\delta^3)$$

$$\frac{d}{ds}\left\langle\frac{xx'}{1+\delta}\right\rangle = \left\langle\frac{x'^2}{1+\delta}\right\rangle + K_{xx}\left\langle\frac{x^2}{1+\delta}\right\rangle - K_{xx1}\left\langle\frac{x^2}{1+\delta}\right\rangle + K_{xx1}\langle x^2\rangle \qquad \frac{d}{ds}\left\langle\frac{x^2}{1+\delta}\right\rangle = 2\left\langle\frac{xx'}{1+\delta}\right\rangle$$

$$\frac{d}{ds}\left\langle\frac{x'^2}{1+\delta}\right\rangle = 2K_{xx}\left\langle\frac{xx'}{1+\delta}\right\rangle + 2K_{xx1}\langle xx'\rangle - 2K_{xx1}\left\langle\frac{xx'}{1+\delta}\right\rangle$$

Truncated set of equations forms closed set.

both methods give nearly identical results for $\langle\delta^2\rangle$ in the regime of interest; similar equations for $\langle x^2/(1-\delta)\rangle$, $\langle xx'/(1-\delta)\rangle$, $\langle x'^2/(1-\delta)\rangle$, and the same set for y; 18 equations total.

Comparison of moment equations with Particle-in-Cell (WARP[1]) simulations (1% velocity spread)

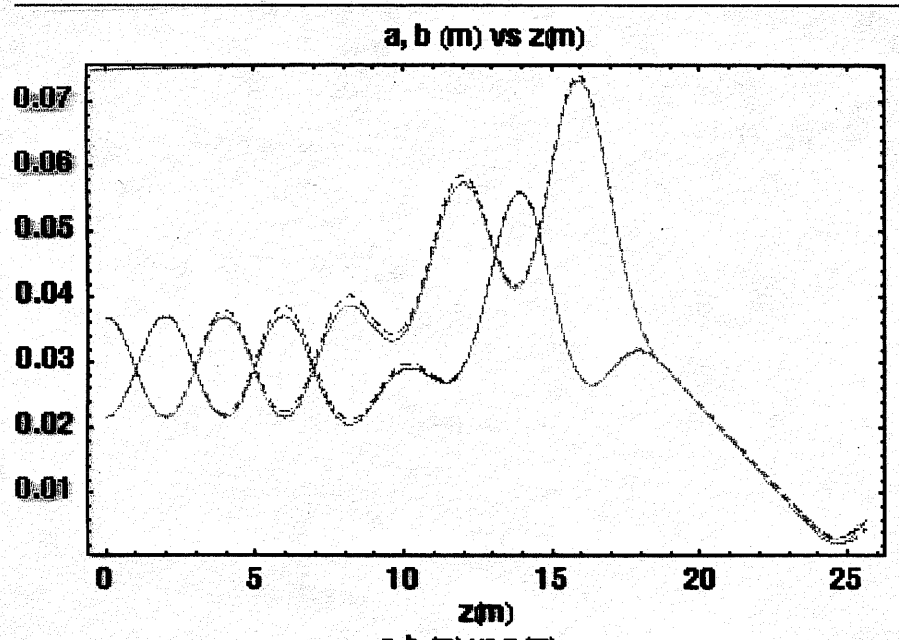

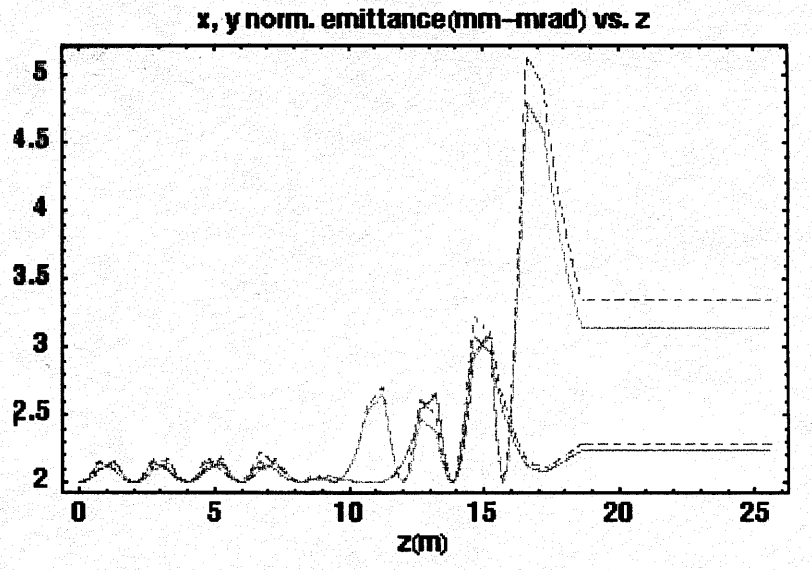

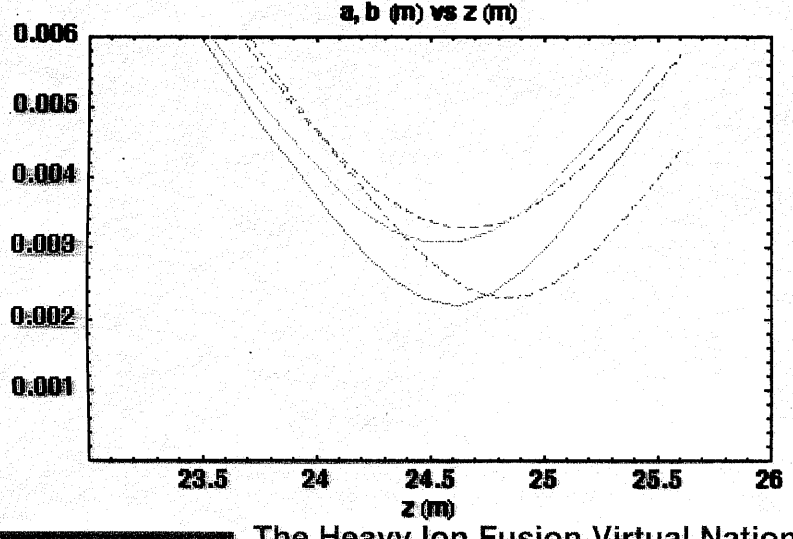

Particle simulations:
Dashed, red (x) and blue (y)
Initial distribution: KV

Moment calcluations:
Solid, magenta (x), and aqua (y)

Comparison of moment equations with PIC simulations (WARP) -- no velocity spread

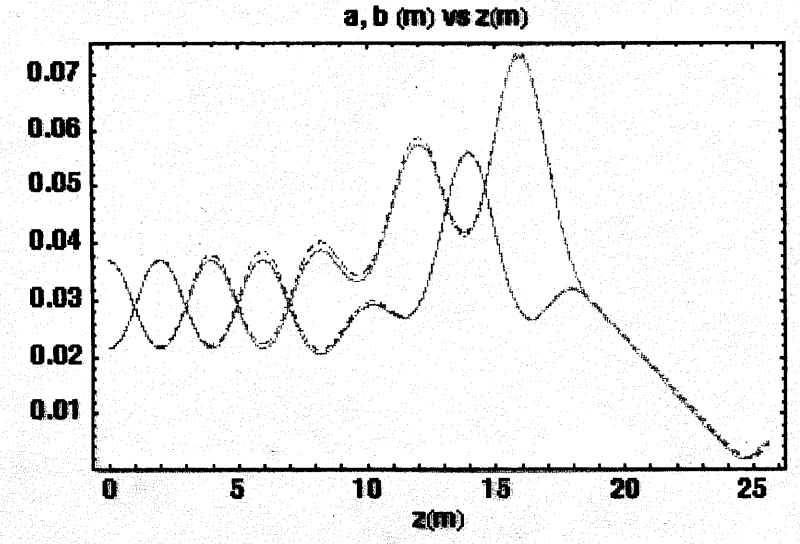

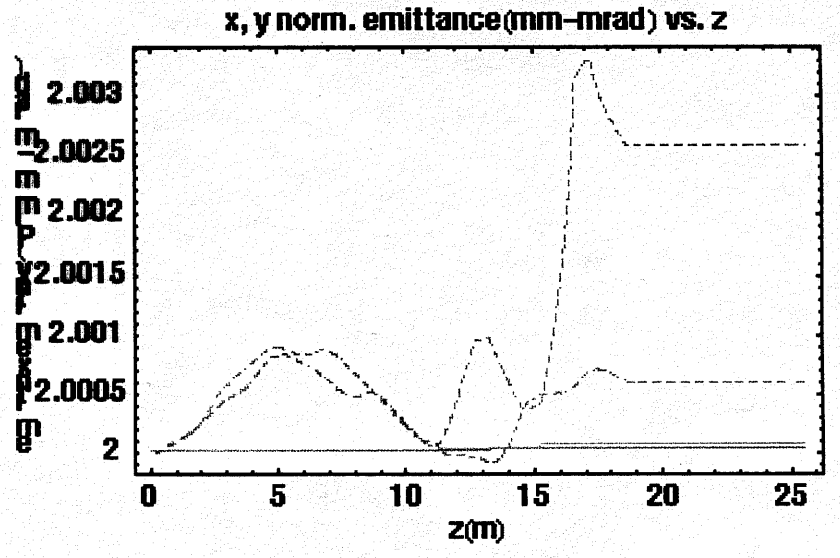

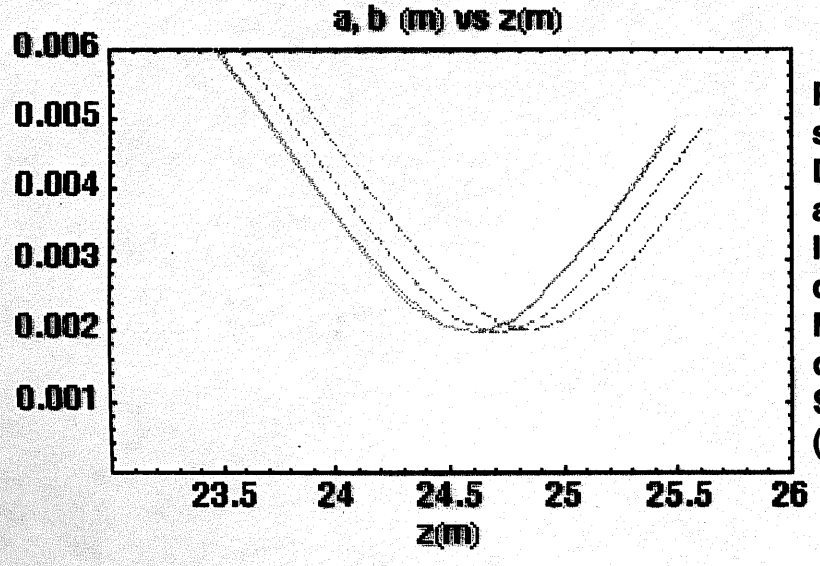

Particle simulations: Dashed, red (x) and blue (y)
Initial distribution: KV
Moment calculations: Solid, magenta (x), and aqua (y)

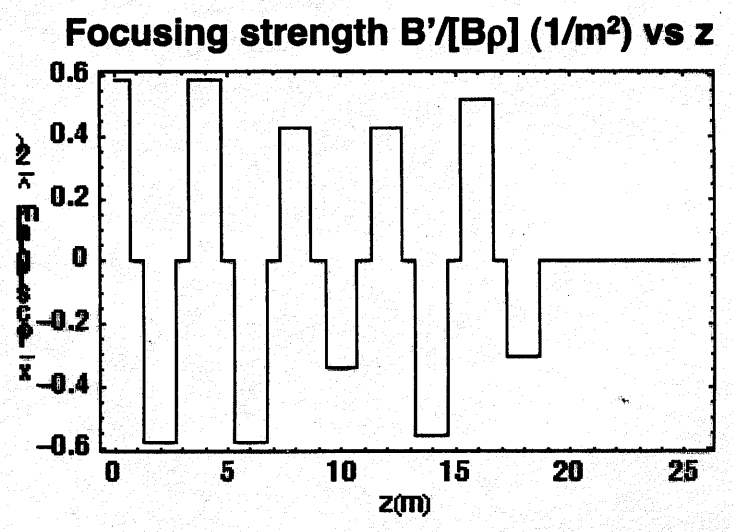

Comparison of WARP results with various grid zoning and particle number (no velocity spread)

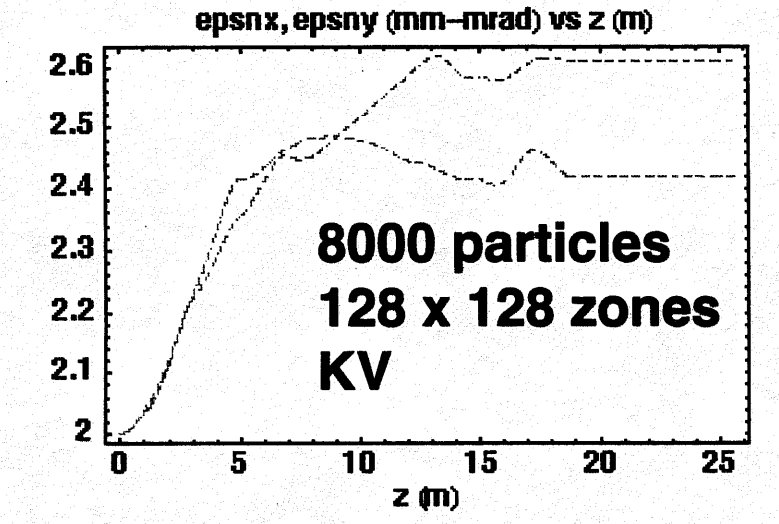

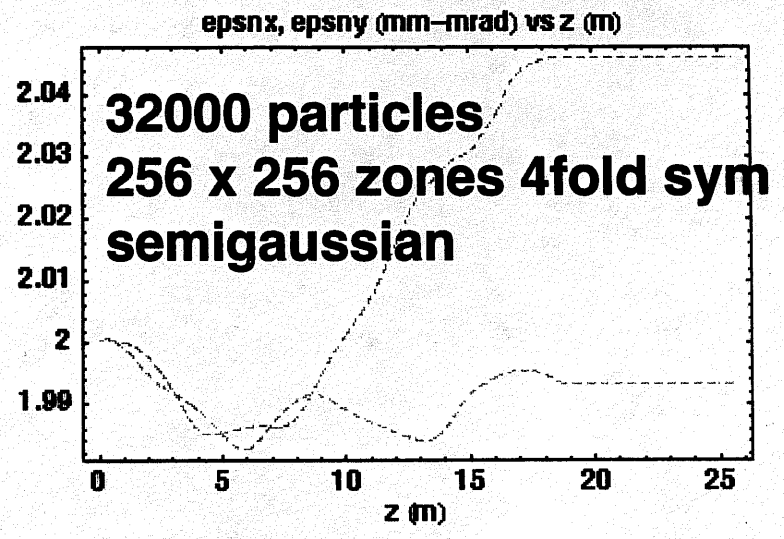

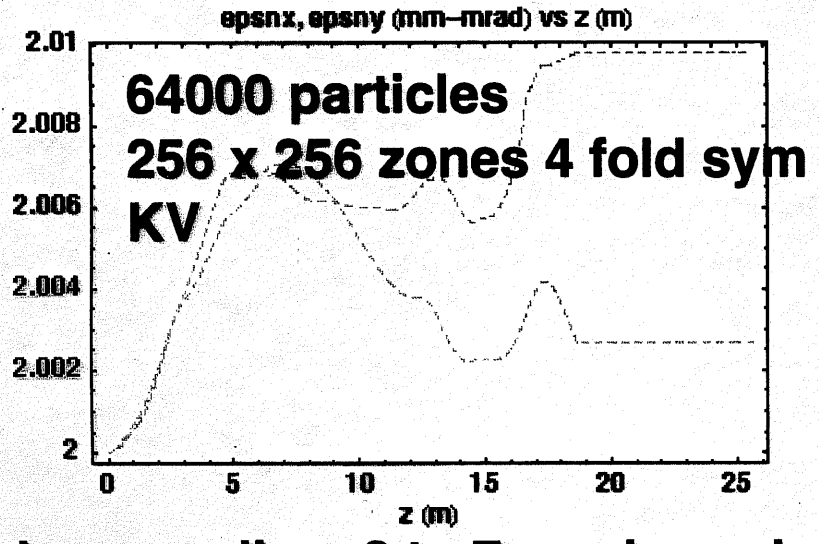

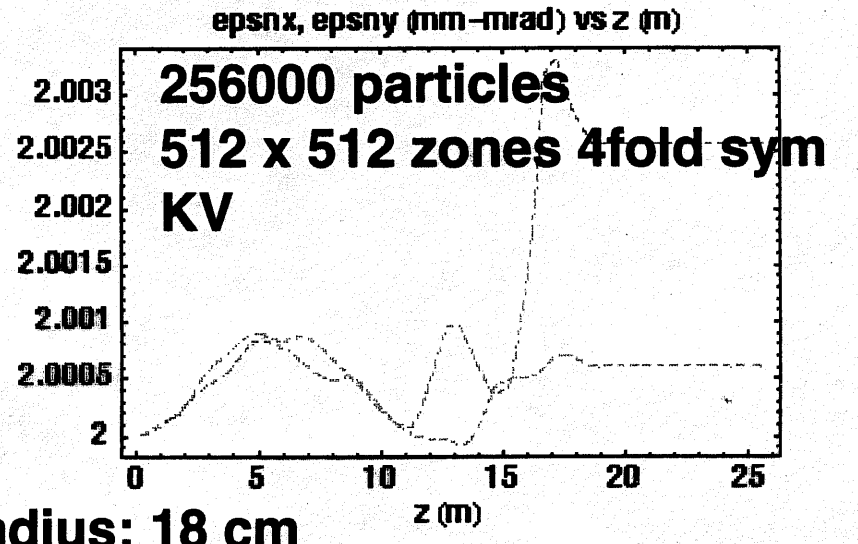

beam radius: 2 to 7 cm, boundary radius: 18 cm

ESTIMATING SPOT SIZE

$$r_x'' + \frac{(\gamma_b \beta_b)'}{\gamma_b \beta_b} r_x + K_x r_x - \frac{2Q}{r_x + r_y} - \frac{\epsilon_x^2}{r_x^3} = 0$$

$$r_y'' + \frac{(\gamma_b \beta_b)'}{\gamma_b \beta_b} r_y + K_y r_y - \frac{2Q}{r_x + r_y} - \frac{\epsilon_y^2}{r_y^3} = 0$$

<u>IN CHAMBER</u>: NO EXTERNAL FOCUSING, NO ACCELERATION AND BEAM IS OFTEN CIRCULAR (BY DESIGN)

$$\Rightarrow \quad K_x = K_y = (\gamma_b \beta_b)' = 0 \qquad \& \quad r_x = r_y = r_b$$

$\Rightarrow$ ENVELOPE EQUATION IS:

$$r_b'' = \frac{Q}{r_b} + \frac{\epsilon^2}{r_b^3}$$

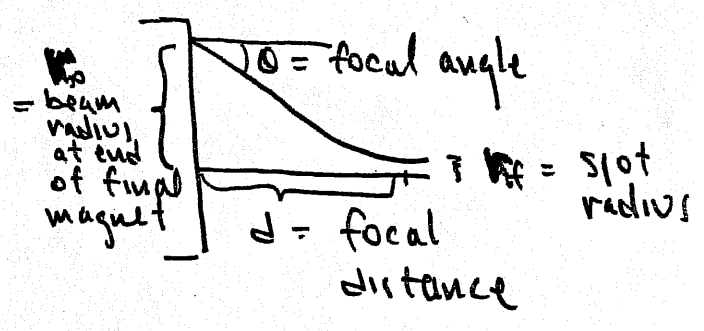

MULTIPLYING BY r_b' & INTEGRATING $\Rightarrow$

$$\frac{r_{bf}'^2}{2} - \frac{r_{bo}'^2}{2} = Q \ln \frac{r_{bf}}{r_{bo}} + \frac{\epsilon^2}{2 r_{bo}^2} - \frac{\epsilon^2}{2 r_{bf}^2}$$

<u>NOW</u> $r_{b\theta}' \cong \theta$ $\qquad r_{bf}$ = spot radius $\qquad r_{bf} << r_{bo}$

$r_{bf}' = 0$ $\qquad r_{bo} \cong d\theta$

$$\Rightarrow \boxed{\theta^2 \cong 2Q \ln\left(\frac{\theta d}{r_{bf}}\right) + \frac{\epsilon^2}{r_{bf}^2}}$$

$$r_{bf} \simeq \frac{\epsilon}{\theta}$$ [when emittance dominates]

$$\simeq \theta d\left[\exp\left(\frac{-\theta^2}{2Q}\right)\right]$$ [when space charge dominates — NOT THE USUAL CASE]

Must also consider contributions from chromatic aberrations, AND OTHER HIGHER ORDER ABERRATION

HEURISTICALLY, THE CONTRIBUTION FROM CHROMATIC ABERRATIONS CAN BE WRITTEN:

$$r_{CHROM}^2 = \alpha^2 d^2 \left(\frac{\delta\gamma}{\gamma}\right)^2 \theta^2 \qquad \text{where } \alpha \sim 6$$

$$\Rightarrow \quad r_{spot}^2 = r_{bf}^2 + r_{CHROM}^2$$

DETAILED simulations or moment-code results REQUIRED TO FIX α.

Accelerator research in the HIF VNL (at LBNL/ LLNL/ PPPL) focuses on three new experiments

1. Ion source/injector:

   High Voltage Source Test Stands (STS-500/100) **(commissioned in December 2001, sited at LLNL)**

2. Acceleration and transport:

   High Current Experiment (HCX) **(commissioned in January 2002, sited at LBNL)**

3. Post acceleration (final focus/chamber transport/drift compression):

   Neutralized Transport Experiment (NTX) **(commissioned in August 2002, sited at LBNL)**

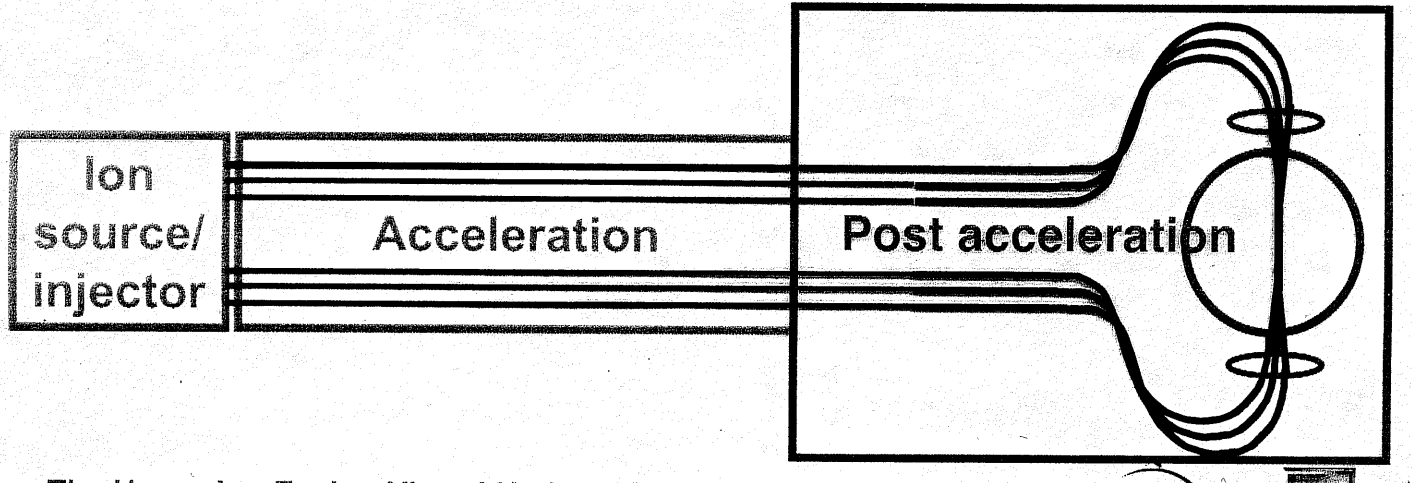

1. Two test stands are being used to study source/injector physics

STS-500

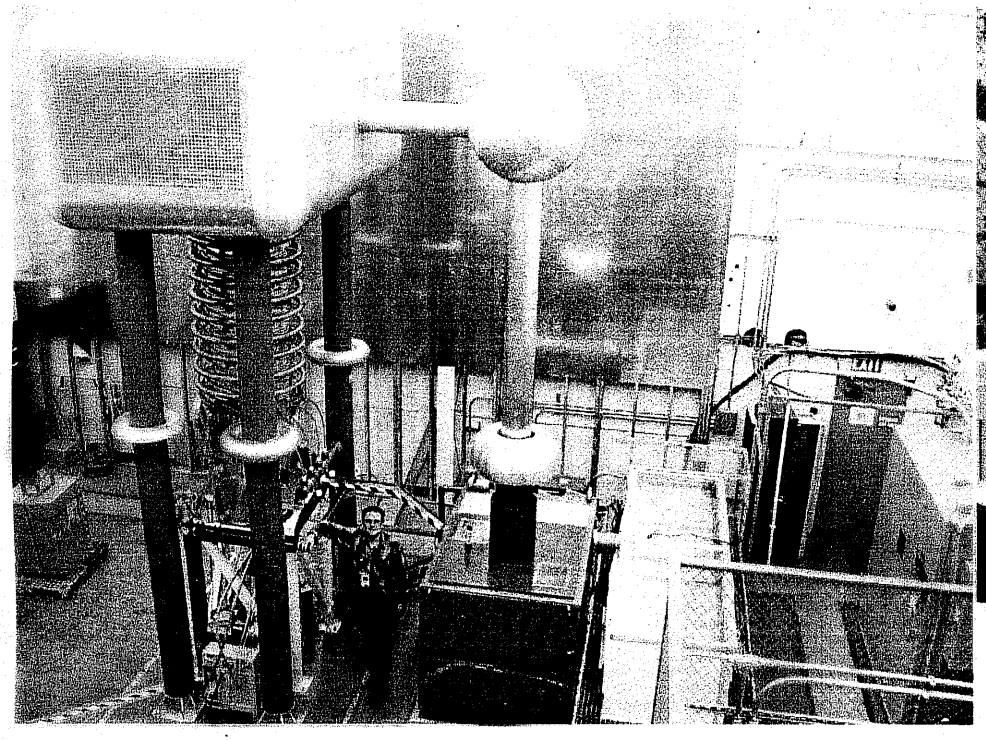

500 kV, up to ~1 A, up to 20 μs
Current research: large aperture sources; aperturing experiments; high gradient insulators

STS-100

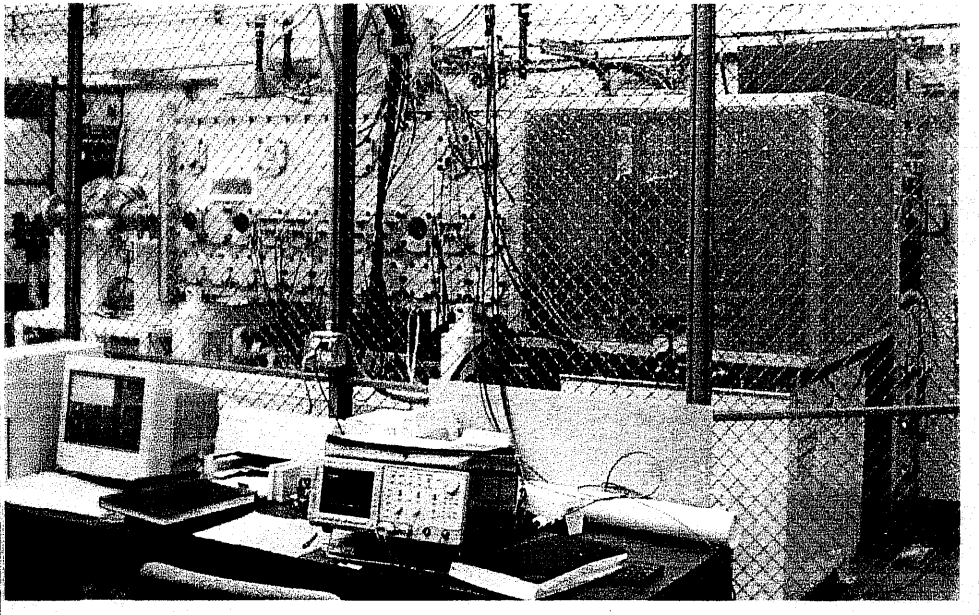

100 kV, ~100 mA, ~10 μs
Ion: variable, currently Ar^+
Current research:
Plasma sources;
Multiple beamlet sources;

Initial kapton image of 61 beamlets shows relatively uniform current density after first accelerating gap

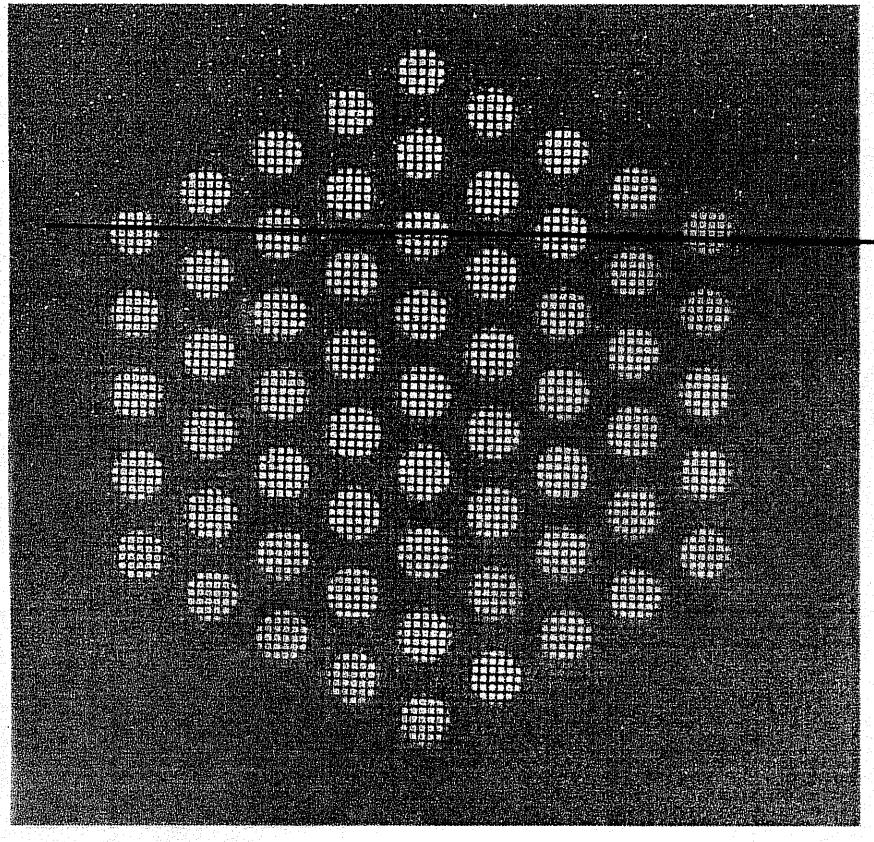

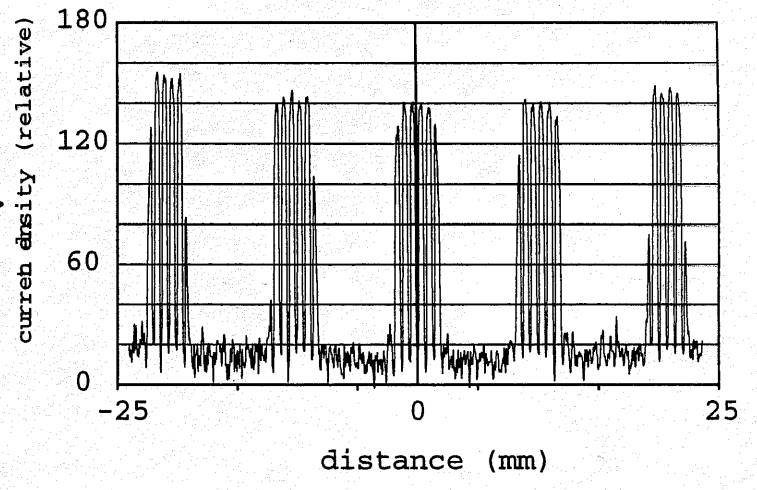

50 kV Ar^+ ions 700 shots

Fine mesh screen in front of kapton

2. HCX is a platform for the study of driver-scale beam dynamics and electron physics

Parameters:
1 - 2 MeV, 0.2 - 0.8 A, 5 μs, K^+

Mission:
To demonstrate beam transport at line charge density **comparable to a** driver
To investigate the effects of electrons, residual gas atoms, and beam/wall interactions **on beam emittance and beam halo**
To establish the "fill factor"

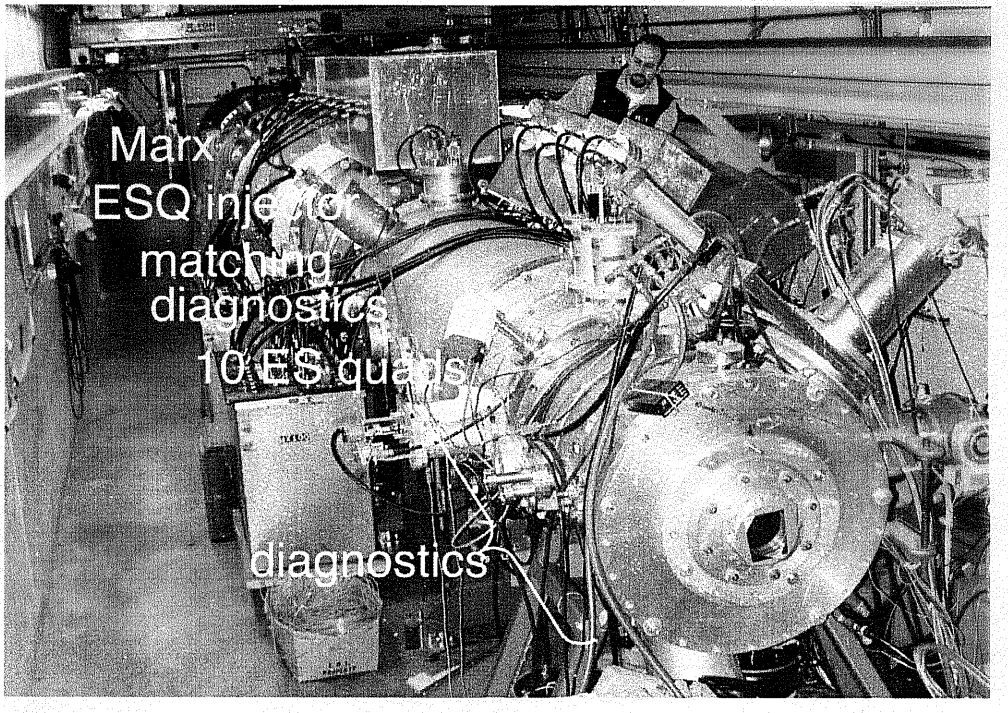

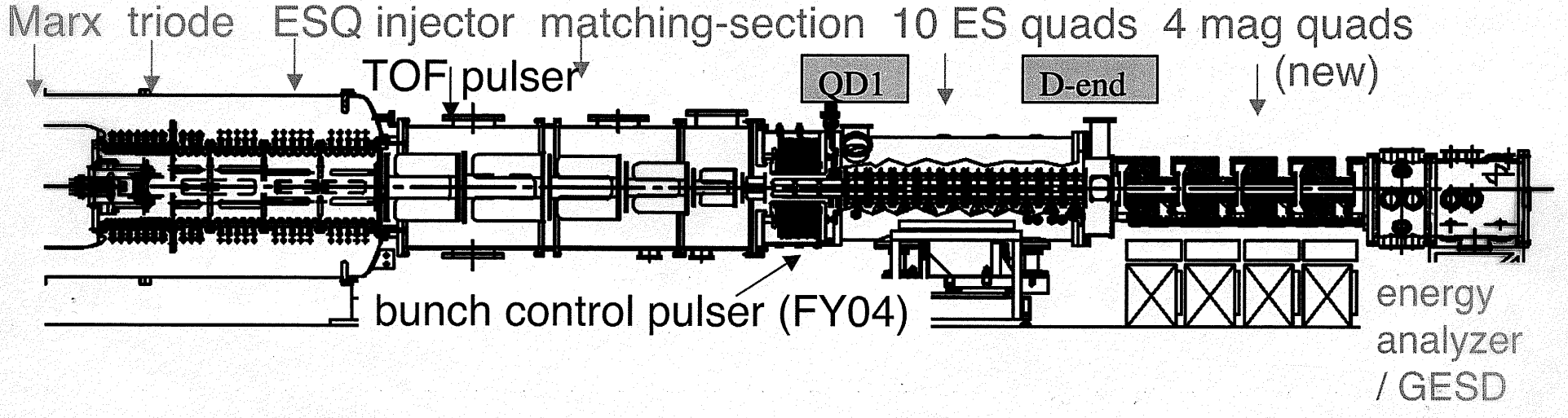

3. Post Acceleration: Neutralized Transport Experiment (NTX)

Parameters: 400 kV, 75 mA, 4 μs, K^+

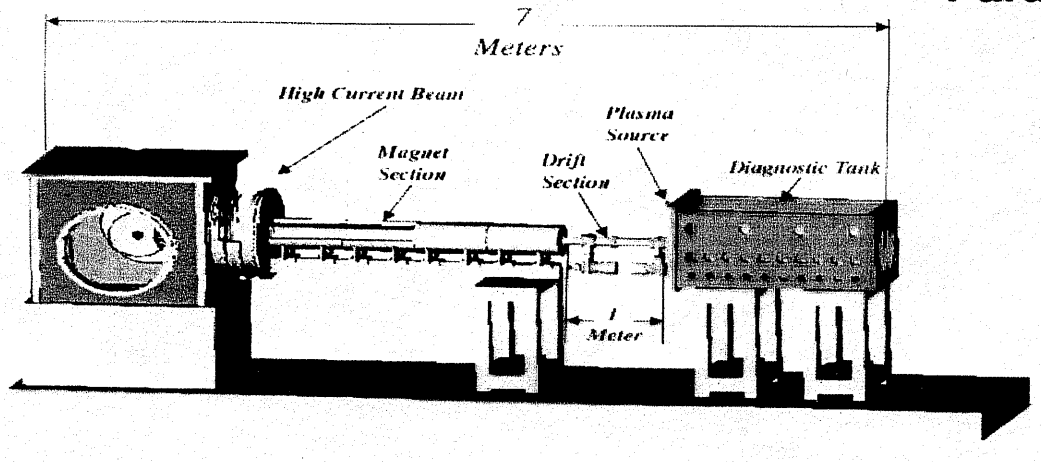

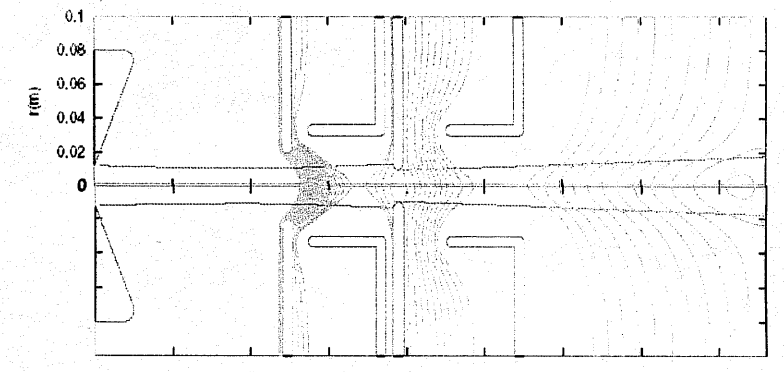

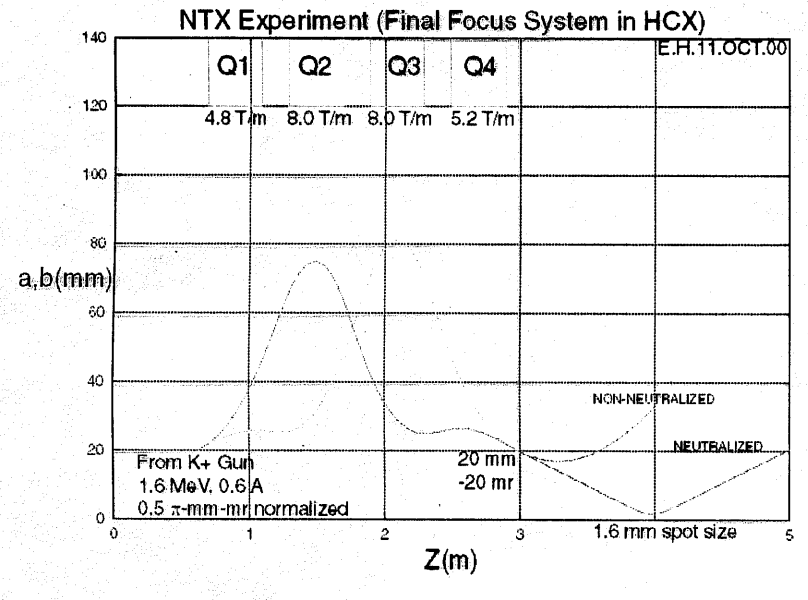

NTX will conduct a scaled experiment with perveance (10^{-4} to 10^{-3}) similar to a driver (Perveance ~ Current/Energy$^{3/2}$)

Simulations predict 99% neutralization

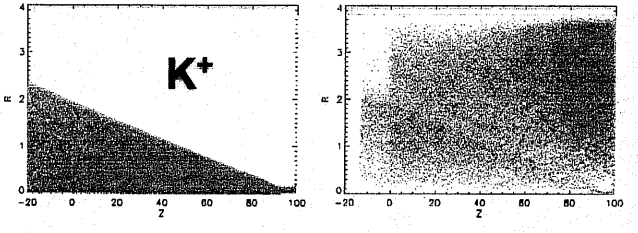

Initial results from NTX show a substantial reduction in spot size with plasma neutralization

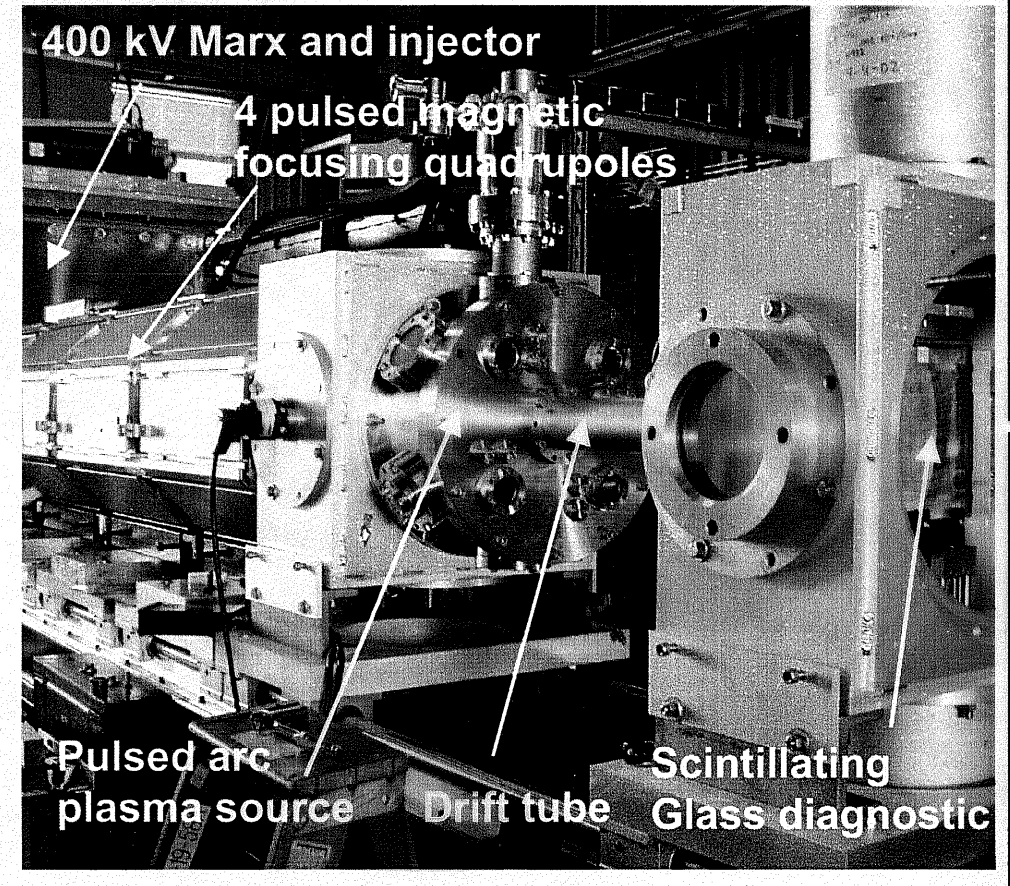

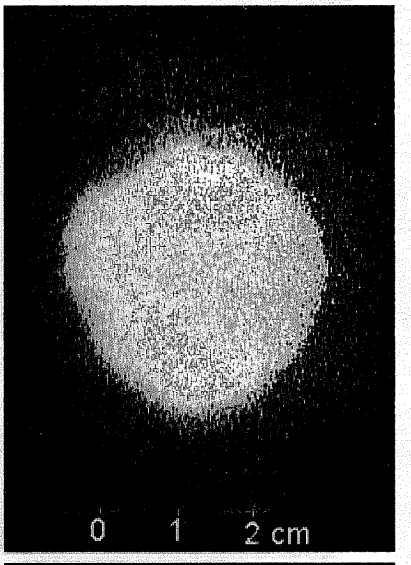

without plasma

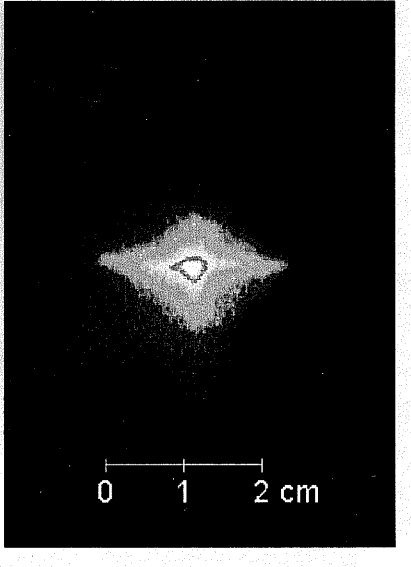

with plasma